

University of Groningen

Cancer Models on Chip

Gil, João Ferreira; Moura, Carla Sofia; Silverio, Vania; Gonçalves, Gil; Santos, Hélder A

Published in:
Advanced materials

DOI:
[10.1002/adma.202300692](https://doi.org/10.1002/adma.202300692)

IMPORTANT NOTE: You are advised to consult the publisher's version (publisher's PDF) if you wish to cite from it. Please check the document version below.

Document Version
Publisher's PDF, also known as Version of record

Publication date:
2023

[Link to publication in University of Groningen/UMCG research database](#)

Citation for published version (APA):

Gil, J. F., Moura, C. S., Silverio, V., Gonçalves, G., & Santos, H. A. (in press). Cancer Models on Chip: Paving the Way to Large Scale Trial Applications. *Advanced materials*, Article e2300692. <https://doi.org/10.1002/adma.202300692>

Copyright

Other than for strictly personal use, it is not permitted to download or to forward/distribute the text or part of it without the consent of the author(s) and/or copyright holder(s), unless the work is under an open content license (like Creative Commons).

The publication may also be distributed here under the terms of Article 25fa of the Dutch Copyright Act, indicated by the "Taverne" license. More information can be found on the University of Groningen website: <https://www.rug.nl/library/open-access/self-archiving-pure/taverne-amendment>.

Take-down policy

If you believe that this document breaches copyright please contact us providing details, and we will remove access to the work immediately and investigate your claim.

Downloaded from the University of Groningen/UMCG research database (Pure): <http://www.rug.nl/research/portal>. For technical reasons the number of authors shown on this cover page is limited to 10 maximum.

Cancer Models on Chip: Paving the Way to Large-Scale Trial Applications

João Ferreira Gil,* Carla Sofia Moura, Vania Silverio, Gil Gonçalves,*
and Hélder A. Santos*

Cancer kills millions of individuals every year all over the world (Global Cancer Observatory). The physiological and biomechanical processes underlying the tumor are still poorly understood, hindering researchers from creating new, effective therapies. Inconsistent results of preclinical research, in vivo testing, and clinical trials decrease drug approval rates. 3D tumor-on-a-chip (ToC) models integrate biomaterials, tissue engineering, fabrication of microarchitectures, and sensory and actuation systems in a single device, enabling reliable studies in fundamental oncology and pharmacology. This review includes a critical discussion about their ability to reproduce the tumor microenvironment (TME), the advantages and drawbacks of existing tumor models and architectures, major components and fabrication techniques. The focus is on current materials and micro/nanofabrication techniques used to manufacture reliable and reproducible microfluidic ToC models for large-scale trial applications.

mortality (10 million). The incidence of cancer is projected to continue to rise, with an estimated 30.2 million new cases by 2040.^[1] This alarming situation prompted the World Health Assembly in 2017 to adopt the “Cancer Prevention and Control through an Integrated Approach (WHA70.12)” resolution, which calls on governments and the WHO to accelerate action plans to reduce cancer-related mortality.

Cancer is defined as the transformation of normal cells into malignant cells due to the alteration of multiple signaling pathways and biomolecular connections. In this context, any cell in the normal organ hierarchy with proliferative capacity can be considered a potential candidate for the origin of cancer if it would allow the sequential accumulation of genetic or epigenetic mutations required for oncogenesis.^[2] Based

on this assumption, it is straightforward to infer that body size and longevity should be directly correlated with cancer mortality. However, recent studies across species revealed that the cancer

1. Introduction

Cancer is one of the most devastating diseases worldwide, with more than 19 million diagnosed cases in 2020 causing severe

J. F. Gil, C. S. Moura
Centre for Rapid and Sustainable Product Development
Polytechnic of Leiria
Marinha Grande 2430-028, Portugal
E-mail: joao.f.gil@ua.pt

J. F. Gil, V. Silverio
INESC Microsistemas e Nanotecnologias (INESC MN)
Rua Alves Redol 9, Lisbon 1000-029, Portugal

J. F. Gil, G. Gonçalves
TEMA
Mechanical Engineering Department
University of Aveiro
Aveiro 3810-193, Portugal
E-mail: ggoncalves@ua.pt

C. S. Moura
Polytechnic Institute of Coimbra
Applied Research Institute
Coimbra 3045-093, Portugal

V. Silverio
Department of Physics
Instituto Superior Técnico
Lisbon 1049-001, Portugal


V. Silverio
Associate Laboratory Institute for Health and Bioeconomy – i4HB
Lisbon Portugal

G. Gonçalves
Intelligent Systems Associate Laboratory (LASI)
Aveiro 3810-193, Portugal

H. A. Santos
Department of Biomedical Engineering
University Medical Center Groningen
University of Groningen
Groningen 9713 AV, The Netherlands
E-mail: h.a.santos@umcg.nl

H. A. Santos
W.J. Korf Institute for Biomedical Engineering and Materials Science
University Medical Center Groningen
University of Groningen
Groningen 9713 AV, The Netherlands

H. A. Santos
Drug Research Program
Division of Pharmaceutical Chemistry and Technology
Faculty of Pharmacy
University of Helsinki
Helsinki 00014, Finland

 The ORCID identification number(s) for the author(s) of this article can be found under <https://doi.org/10.1002/adma.202300692>

© 2023 The Authors. Advanced Materials published by Wiley-VCH GmbH. This is an open access article under the terms of the Creative Commons Attribution License, which permits use, distribution and reproduction in any medium, provided the original work is properly cited.

DOI: 10.1002/adma.202300692

mortality risk is largely independent of both body mass and adult life expectancy components, as stated by Peto's paradox.^[3] This is a remarkable example of how our current knowledge of cancer represents only the tip of the iceberg.

The hierarchal organization of tumoral cells promotes the formation of tumoral tissues in primary homing organs, which, in advanced disease development stages (metastases) have the potential to spread to secondary organs. Additionally, it was observed that normal tissue adjacent to the tumor (NAT) presented substantial phenotypic and genetic changes.^[4] Tumor tissues present a marked heterogeneity between individual tumors (intratumoral heterogeneity) or even when occurring in the same organ (intertumoral heterogeneity) in terms of their molecular profiles, as well as their morphology and the expression of specific markers (such as hormone and growth-factor receptors). Indeed, the contribution of the genetic mutational profile to the tumor phenotype, as well as the relationship between the cell of origin and the cancer stem cell, remain substantially unknown.

The genomic stratification of cancer by integrative multi-omic approaches provides a realistic perspective on network-level alterations for the development of more effective therapeutic strategies to address cancer heterogeneity.^[5] Classifying tumors into subtypes based on their biological hallmarks has contributed to a certain extent to a more accurate prediction of their evolution and the implementation of proper therapeutic plans.^[6] The Pan-Cancer Analysis of Whole Genomes Consortium and The Cancer Genome Atlas permitted the reconstruction of the life history and evolution of mutational processes and driver mutation sequences of 38 cancer types.^[7] However, the implicit assumption of sample assignment to a particular cluster or group of patients is an inherent flaw in this approach.^[8]

Molecular heterogeneity among tumor subtypes may result in distinct signaling alterations in response to the therapeutic strategy, allowing tumor recurrence and the dissemination of metastatic tumors. Even though less than 0.1% of tumor cells metastasize, they are considered the main cause of cancer mortality.^[9] According to Steeg et al., metastases are responsible for over 90% of the mortality of cancer patients.^[10] A recent study, based on data from 2005 to 2015 from the Cancer Registry of Norway, revealed that 66.7% of cancer deaths were attributed to metastases.^[11]

The complexity of the tumor microenvironment, which includes cancerous cells, lymphocytes, macrophages, blood vessels, and the extracellular matrix (ECM), as well as combining several biophysical and biochemical mechanisms, constitutes an intricate paradox in cancer research. Deconstructing the complex TME to its building blocks became critical for elucidating the basic mechanisms of the dynamic interactions of cancer cells with their microenvironment, consisting of stromal cells and ECM components, which were essential to decoding cancer cell progression and metastasis and identifying clear multidrug resistance factors and opportunities for successful therapeutic interventions.^[12]

2D cell models have provided the foundation of cancer research for many years. Though they present severe limitations in terms of mimicking the real features and complexity of the 3D TME regarding cell-to-cell interactions and the influence of the ECM. Multicellular 3D models become an excel-

lent tool to bridge the gap between oversimplified 2D systems and unrepresentative animal models, allowing novel insights into the biology of cellular interactions and communicating within the TME using highly tractable, physiologically relevant systems.^[13,14]

ToC is 3D tumor model produced in microfluidic devices to mimic important features of the tumor physiology (**Figure 1**).^[15] ToC technology has been offering a practical way to build patient-specific tumor models used in fundamental research on the biophysical characteristics of tissue, in the development of diagnostic tools, and in the design of therapeutic approaches, to mention a few. To achieve true functioning microtissues, however, the ECM, a variety of cell types, and vasculature with intricate spatiotemporal distribution must be integrated into the ToC. This technology will be able to offer essential knowledge that enables correlation between the structural characteristics of the tumor and its growth and severity. The 3D tumor models have the potential to replace standard in vivo assays, which are expensive, time-consuming, and have serious ethical implications, while enabling higher-throughput screening of early-stage anti-cancer therapies.

1.1. Current Challenges to Replicate the Complexity of Tumor Microenvironments

Cancer diagnosis and therapy have been severely limited by the ability of drugs to reach the tumor and diffuse homogeneously through the tumor tissue.^[16–18] The main cause of failure in drug diffusion into tumoral tissue is primarily due to the highly complex architecture of tumors and, in particular, a lack of understanding of the structural properties and biochemical and biophysical mechanisms that govern the TME.^[19] TME hallmark features consist of a complex and dynamic network of ECM proteins and biochemical/ biophysical factors embedded with cells, namely endothelial cells, cancer-associated fibroblasts (CAF), pericytes, and several infiltrating immune cells.^[12] However, it is important to point out that the TME architecture and composition present significant changes depending on tumor type.

The dynamic interactions in the TME regulate and define the tumor cascade. These interactions control cell proliferation, migration, differentiation, cytoskeletal organization, and its consequent cell signaling.^[20] The communication between all these tumoral entities is mainly governed by chemokines, growth factors, enzymes, extracellular vesicles, and/or mRNA.^[21] Additionally, TME influences tumor genesis, growth, and progression in a variety of ways, including by triggering angiogenesis and metastatization, causing drug resistance, and inhibiting the immune system (**Figure 2**).^[22] Indeed, the increasing significance of TME in cancer biology has recently shifted cancer research and treatment from a cancer-centric model to a TME-centric one.^[23]

1.1.1. Dynamics in Tumor Microenvironment

The TME is crucial to tumorigenesis because it contains tumor cells that interact with surrounding normal cells in a way that enables the tumor's growth and progression. Non-malignant

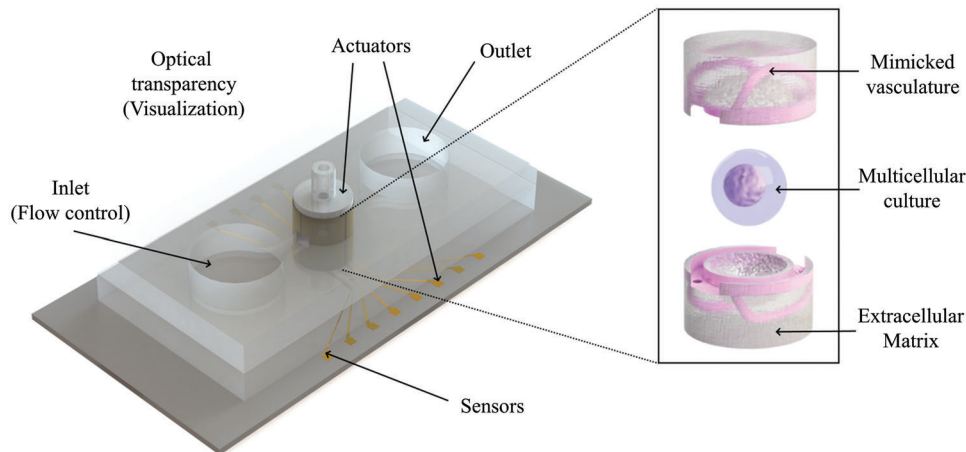


Figure 1. Schematic of a ToC device integrating multiple features necessary for their application as tumor models.

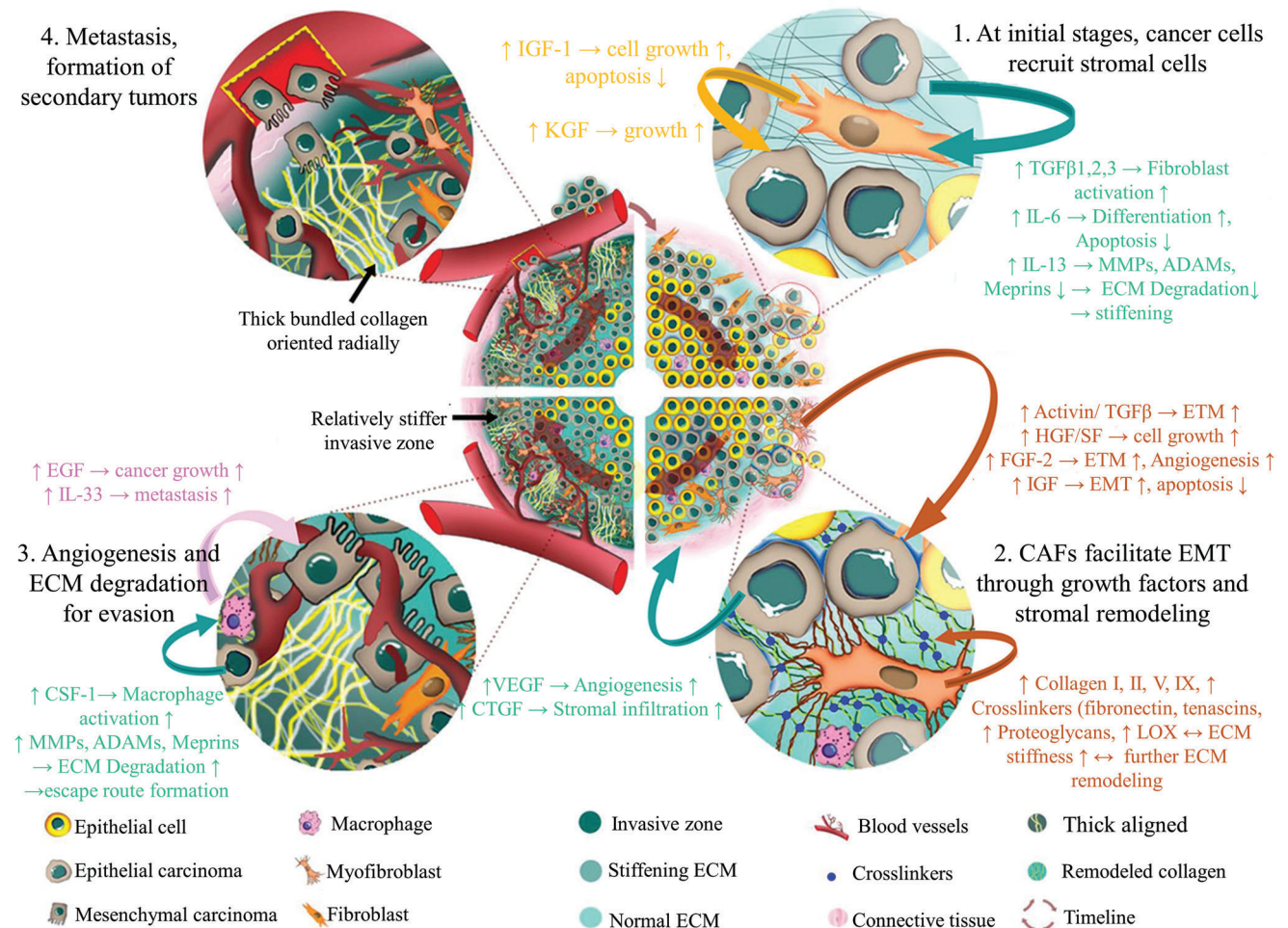


Figure 2. The role of stromal cells in promoting cancer progression. During carcinogenesis, cancer cells recruit stromal cells from nearby tissue. The dynamic interaction between stromal and cancer cells in the TME induces tumor development. Endothelial cells, fibroblasts, adipocytes, and stellate cells are all components of the stromal architecture, which changes depending on the type of tumor. Through the release of growth factors and cytokines, the TME controls angiogenesis, proliferation, invasion, and metastasis. Adapted under the terms of the CC-BY Creative Commons Attribution 4.0 International license (<https://creativecommons.org/licenses/by/4.0>).^[29] Copyright 2018, The Authors, published by Elsevier on behalf of Research Network of Computational and Structural Biotechnology.

cells in the TME also play a significant role in all stages of this process.^[24] These cells can be recruited by the tumor and are present throughout the tumor's growth and progression.^[25] A series of gradients are created in the TME as a result of it being a multicellular environment with an external ECM. The synthesis of ECM is regulated by tumor cells, mutated genes, signaling pathways, and transcription factors, which makes it susceptible to all the components of the TME and, like the other components, heterogenic. Stroma cells, as an example, have mechanisms for the constant rebuilding and remodeling of the ECM, and it is through the ECM that crosstalk between these cells occur.

The ECM, comprised of soluble components and a network of biopolymer fibers made of proteins, proteoglycans, glycosaminoglycans, and glycoproteins varies in content and structure depending on the tissue. Mechanical properties, as well as morphology, porosity, and mesh size, are determined by the size and density of these fiber networks. The spatial organization of this network controls communication due to its elasticity, which is dependent on the biophysical features, while allowing the matrix to move and contract. The presence of the molecular components indicated above, as well as the resulting pore size, viscoelasticity, cross-linking, cellular density, and interstitial pressure, impact ECM stiffness, promoting tumor cell reprogramming.^[26]

The following examples illustrate dynamics in the tumor environment. Matrix metalloproteinases (MMP) are essential for ECM degradation and tumor cell invasion and are the main enzymes involved in ECM degradation. Besides, high expression of protease inhibitors correlates with tumor reduction, whereas high MMP correlate with tumor growth.^[27] Generally, the activation of CAF stimulates tumor progression. CAF overproduction of ECM proteins forms an anomalous ECM, which prompts the immunosuppression of tumor cells. Tissue fibrosis and the increase in matrix stiffness lead, via various physicochemical pathways, to epithelial cellular transformation and hyperplasia. In addition, CAF promotes tumor cell proliferation and metabolism by inducing angiogenesis and oxidative stress, which induces the autophagy pathway.^[12] Pericytes and endothelial cells constitute and modify the basement membrane, either in the angiogenesis or tumorigenesis processes. Pericytes have mechanisms to attract and regulate the passage of cells through the membrane and endothelial cells are part of the inner layer of blood vessels. Alterations to the phenotype of endothelial cells occur during tumorigenesis. These tumor-derived endothelial cells promote vascular leak, high interstitial fluid pressure, reduce blood flow, and tumor hypoxia and acidosis.^[12] Tumor-associated immune cells can circulate and infiltrate the tumor tissue and remodel other immune cells into tumor-derived ones. Additionally, they also provide motility and metastatic ability to tumor cells by producing migration-stimulation factors. This event, along with endothelial cells and pericytes being compromised, will enable tumor cells to move into the endothelium and form circulating tumor cells (CTC). CTC, soluble factors, cfDNA, and/or exosomes from the primary tumor travel through the blood stream and may produce changes in the ECM at a distant site or alter the phenotype of a healthy cell, creating a chain reaction that leads to the development of a metastatic site.^[28]

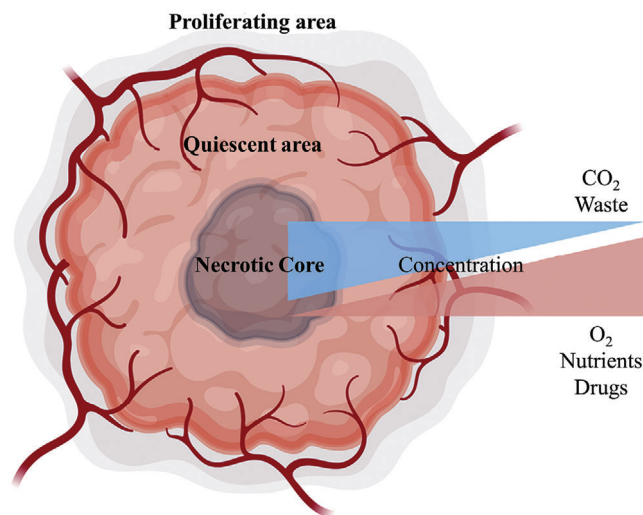


Figure 3. Tumor architecture in relation to extracellular gradients. The majority of solid tumors are arranged into 3D structures consisting of an inside core with a high percentage of necrotic cells, an outside region with proliferating cells, and a quiescent area. Created using Biorender.com.

1.1.2. Heterogeneity of Tumor Microenvironment

The concentration of oxygen, nutrients, pH, and drugs is often highest in the outer zones and lowers as they diffuse inside the tumor mass. While waste and carbon dioxide can easily pass from exterior cells into the surrounding TME, they are substantially concentrated inside the tumor mass (**Figure 3**). Tumor cells have sensing pathways that allow them to monitor their environment and constantly adjust their metabolism while escaping immunosurveillance or therapeutic interventions.^[30] As a result, cancer cells must compete with stromal cells for resources to proliferate.^[31]

The cellular/immune niche as well as the ECM architecture are both shaped by the metabolic interactions between cancer cells and the surrounding microenvironment, which alter the proliferation and aggressiveness of tumor cells. These interactions generate an intricate set of metabolic pathways that contribute to the active modification of the TME, including angiogenesis, dysregulation of the immune system, and remodeling of the ECM. In this same process, tumor cells undergo changes at the phenotypic and genotypic levels. These mutual alterations impact heavily on the evolution and progression of cancer. Either in different anatomic locations or within the same tumor, significant spatial and temporal heterogeneity is identified in the genetics of tumor cells.^[32]

The tumorigenic cascade, originated by an accumulation of dysregulations in a series of events, generates physical and chemical properties on the TME, creating dynamic reciprocity between neoplastic cells, stromal cells, micro-vascularization, innervation, ECM scaffolding, bioelectric fields, and soluble factors of tumor growth control.^[26] The factors that generate tumor heterogeneity and its spatiotemporal evolution remain largely uncharacterized. A detailed tumor heterogeneity review is presented elsewhere.^[32,33]

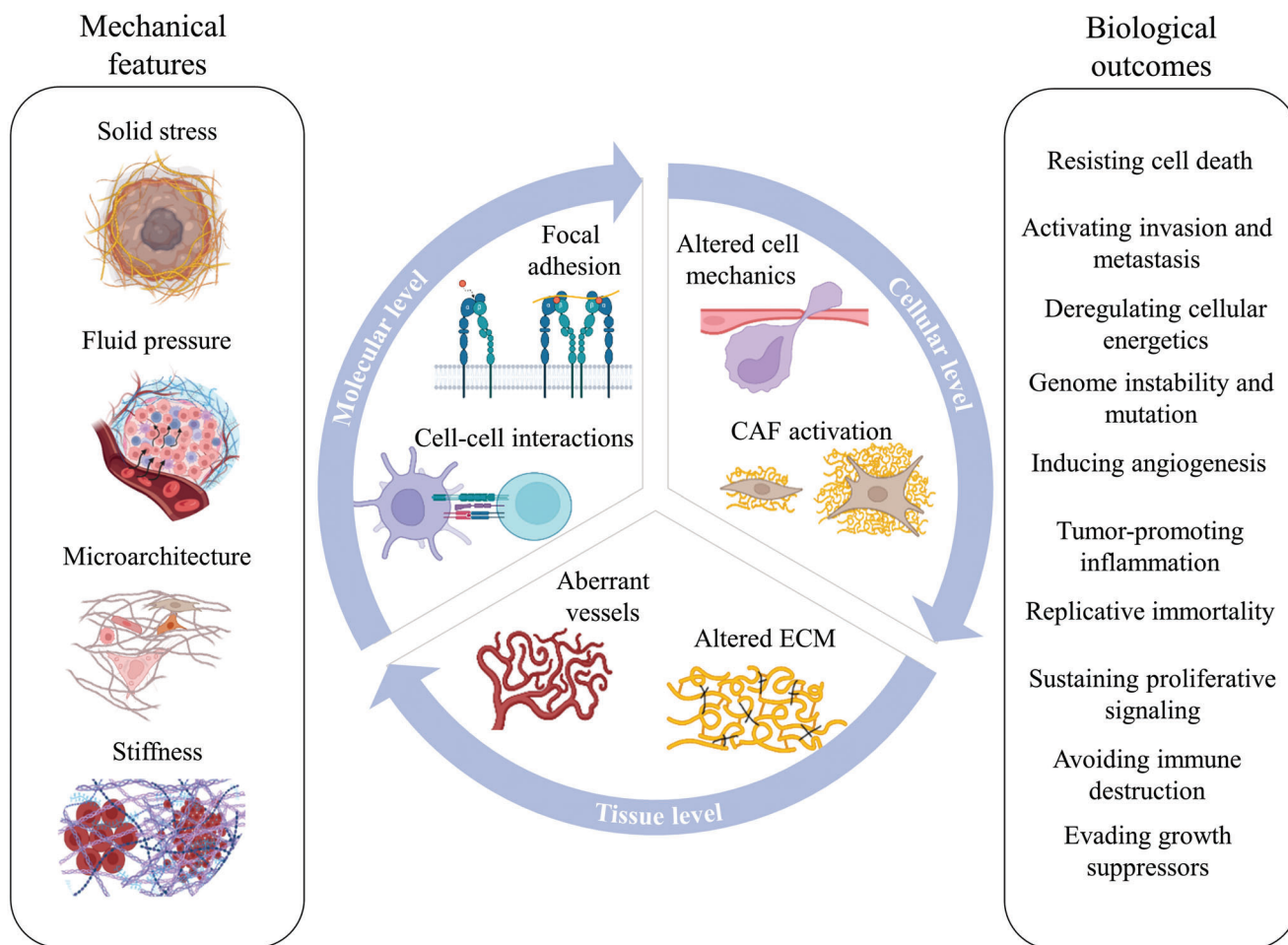


Figure 4. Physical characteristics of the tumor that can generate effects across the molecular, cellular, and tissue levels of the tumor and examples of outcomes produced by biophysical interactions that affect the tumor prognosis. Created using Biorender.com.

1.1.3. Biophysical Signaling Pathways

In recent decades, cancer research has focused primarily on the study of the influence of extra- and intra-cellular biochemical signals in order to comprehend cancer cell proliferation, invasion, and metastization. Recently, a paradigm shift in research allowed researchers to discover that biophysical signals can be converted by cells into biochemical signals via mechanotransduction mechanisms, which affect cell behavior such as genetic expression, phenotyping, and differentiation.^[34] Mechanotransduction begins with a mechanical signal generated locally and relayed across the cytoskeleton network. Mechanical stimuli produce cellular structural deformation if the forces are substantial and are transmitted for a long enough period of time. The conformational changes are followed by the selective activation of intracellular biochemical signaling processes. The cytoskeletal components and those of the cell membrane are then the primary systems for assisting in the transmission of a complete set of chemical and physical signals that produce a regulated mechanoreponse that determines the cell's prognosis.^[35] In fact, tumor cells are highly susceptible to mechanical stress, from tension (ECM/cells interaction), compression (tumor expansion in a con-

finied space) to shear (blood and interstitial fluid), which allow the reprogramming of the cellular response, promoting biological phenomena that are closely related to tumor progression and aggressiveness.^[36] Cell adhesion, motility, and proliferation are also significantly influenced by the biophysical factors that preserve a tumor's structural integrity. In addition to producing nutrient/growth factor gradients, a stromal/ECM barrier or tumor cell location within the TME may also act as a source of exogenous physical forces that may reconfigure tumor cells and potentially act as a defense against cancer therapy, and the destruction of adaptive immune cells or even stromal stiffness can induce normal epithelial cells to develop malignant phenotypes (Figure 4).^[37] A fundamental question that still needs to be answered is how and why biomechanical stimuli work in this wide range of biological settings and what the key signaling pathways are that control the growth and spread of tumors. In vivo studies carried out so far have revealed great technical difficulties in unraveling the influence/contribution of biochemical and biomechanical signals.^[38]

This review provides a deep overview of fabrication processes, design, and integration of sensorial and actuation systems, as well as tumor biofabrication, while demonstrating the

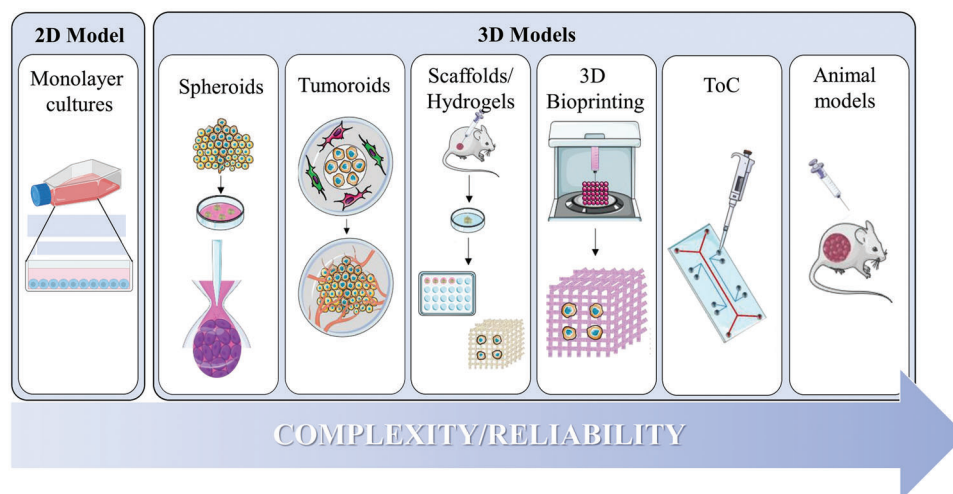


Figure 5. Overview of different tumor models. Adapted under the terms of the CC-BY Creative Commons Attribution 4.0 International license (<https://creativecommons.org/licenses/by/4.0>).^[46] Copyright 2021, The Authors, published by Frontiers.

advantages of ToC technology and contributing to a more effective and precise understanding of tumor behavior. Additionally, it will present an exhaustive reflection on the identification of the challenges for the efficient translation of ToC technology to produce real-mimicking, high-throughput, and reproducible in vitro models that can successfully reach the pharmaceutical industry.

2. Tumor Models

Tumor models serve as tools to tackle the main challenges in cancer research by efficiently establishing in vitro tumor microenvironments able to physiologically mimic tumoral tissues. These models have been extensively developed and explored as efficient means for fundamental studies of biological structure and biophysical and biochemical factors related to the multistep progress of tumors, screening anticancer drugs to reveal the nature of cancer, and predicting more realistic therapeutic plans.^[39]

Nowadays, these studies are made either by conventional 2D tumor tissue monolayers, 3D cultures, or in vivo trials.^[13,40,41] On one hand, the conventional 2D-cultures are somehow oversimplified, and even though they have given some insight into tumor cell interactions in the past, they lack representation of the complex architecture and microenvironment of the tumor (**Figure 5**). On the other hand, 3D cultures can better mimic tumor cell–cell interactions and topography by allowing the definition of geometry, cell heterogeneity, biophysical cues, transport, and stimulation.^[42–44] Animal models are still the gold standard since they can emulate the complexity of the whole organism. However, their significantly different genomes, anatomy, and physiology, as well as their immunological and inflammatory responses, will provide outputs that fail to hold true for humans.^[63] Recently, to better recapitulate the stochastic nature of human cancer, chimeric mouse tumors have been explored.^[45] Although this approach still raises significant ethical issues, chimeric mouse tumor models reveal low consistency in terms of reproducibility.

With the recent developments of lab-on-a-chip technology and its further applications in organ tissue engineering, it is expected

that ToC will compete with the present state-of-the-art tumor animal models, avoiding ethical issues related to the use of animal models and delivering human-relevant information.^[47] In contrast with animal models, ToC can be fully composed of human-derived cells. Taking advantage of microfabrication techniques, microfluidics, and TE, ToC is being engineered to model the main functions of tumor physiology. Highly integrated ToC devices are composed of microfluidic chips, cells/microtissues, and biomaterials; microactuators for physical and chemical stimuli; and microsensors for monitoring the status of cells. The microfluidic chip provides cells with confinement and allows them to move in the interstitial environment. This way, motile cells like immune cells or CTC can mimic in vivo behavior. Together with biomaterials and microfabrication techniques, multiple cell types can be arranged in complex spatiotemporal architectures. Co-culture of healthy tumor-associated and immune cells can be done and combined to form a vascular system inside the same device. The right choice of materials and techniques allows the reproduction of several TME conditions.^[39] Biochemical gradients, dynamic multicellular and matrix interactions, and biomechanical stimulation at a human-relevant level are examples of features that ToC technology can provide within the same model. This section presents the advantages and disadvantages of the different tumor models and summarizes them in **Table 1**.

2.1. 2D In Vitro Cell Models

The easiest, cheapest, and highest-throughput tumor model capable of being produced at the moment is to grow 2D cell monolayers in plastic dishes. Despite the growing number of proofs that cell morphology, differentiation, proliferation, viability, metabolism, and gene expression are remarkably different from the in vivo environment, many of the therapeutics tested for the treatment of tumors are still performed in these 2D models.^[40]

The 3D structure of in vivo tumors makes cell–cell and cell–matrix interactions respond in a different manner than in a 2D

Table 1. Advantages and disadvantages of tumor models.

Tumor models	Advantages	Disadvantages	Ref.
2D cell cultures	Inexpensive Well established Convenient Easier cell observation and measurement	Not representative of real cell environments Reduced cell–cell interactions	[40,49]
Spheroids	Growth factors and ECM are not required Allows for cell co-culture Cross-linking methods are not necessary Cost-effective and simple	Simple and weak structure Homogenous spheroids are challenging to construct Lack of vasculature Limited size and lifetime	[53,54]
Tumoroids	Conserves tumor heterogeneity Requires ECM Reproduction of cell-ECM and intercellular interactions	Difficult to replicate the gradient of gases, nutrients, and pH Requires ECM cross-linking Lack of vasculature	[58,59]
Scaffolds/ Hydrogels	Amenable to high throughput screening High reproducibility Co-culture ability	Simplified architecture Can be variable between models	[60]
3D Bioprinting	Custom-made architecture Chemical, physical gradients High-throughput production Co-culture ability	Challenges with cells/materials Difficult to be adapted to high throughput screening Issues with tissue maturation	[65,66]
Animal models	Efficacy Drug resistance Whole-body physiology TME mimicry Genetically modifiable	Unable to upscale Different pathophysiology to humans Costly Ethical issues	[70,75]
ToC	Microarchitecture In vivo-like microenvironment gradients Biophysical stress Reduced volumes of samples Good visualization capabilities Integrated sensory and actuator capabilities	Not standardized or automatized Complex experimental set-up Need for integrated platforms	[39,50]

monolayer.^[48] Besides, the heterogeneity of cells, substrate topography, stiffness, architecture, and physicochemical stimulation are completely different between the two.^[49] 2D models, due to their lack of heterogeneity, generate changes to the original tumor phenotypes.^[50] Moreover, they still lack the immune interactions and drug barriers found in *in vivo* tumors, making them inappropriate for drug testing. These 2D models lead to a series of false-positive selection of drugs due to the lack of environmental cues in *in vivo* tumors, which affect not only the natural responses of cells but also the responses to said drug.^[40]

2.2. 3D In Vitro Cell Models

The limitations of 2D cell culture models gave rise to the development of 3D models, which resulted in a better mimicking of the cellular microenvironment of native tissues. Spheroids, organoids, and 3D bioprinting technologies are, among others (Figure 5), the most used approaches to producing 3D models that have been gathering attention for *in vitro* tumor recreation.^[46,51,52]

Spheroids are aggregates of cells grown in suspension or embedded in a 3D matrix to produce 3D models capable of recapitulating cell–cell and cell–ECM interactions.^[53] They can be produced using different methodologies, like the hanging drop

technique, spinner flasks, ultra-low attachment plates, or micro-patterned plates, to name a few.^[40] Spheroids are often employed for drug screening, investigations of tumor development and proliferation, immunological interactions, studies of invasion, matrix remodeling, and angiogenesis, despite being more expensive and time-consuming than 2D cell culture.^[54] These models have been evolving, and through their 3D conformation, the possibility of co-culture and embedding in a matrix makes them more suited as tumor models than 2D cultures.^[55] Upon their growth, a gradient of oxygen and nutrients appears, resulting in a core under hypoxic conditions, bringing the protein and gene expression profiles of tumor cells in spheroids substantially closer to the clinical and *in vivo* gene expression profile.^[54] However, due to the absence of stromal cells and the effects they have, important elements of the tumor environment are not duplicated inside spheroid aggregates. Multicellular tumor spheroids are being developed to address these limitations.^[56,57] Key advantages of spheroids and hanging drops are their cost effectiveness, high throughput, repeatability, and simplicity of usage.^[46]

Organoids, which were originally employed for stem cell research, have been used for cancer research and are known as tumoroids.^[58] They usually derive from tissue-specific stem cells or progenitor cells and are most frequently grown on a scaffold-based system.^[59] Organoids are cell-based structures that, like spheroids, primarily rely on the capacity of cells to form and

arrange themselves into 3D structures (Figure 5).^[59] These allow for the exploitation of co-cultures as well as the reproduction of interstitial fluid pressure conditions. As they can replicate not just the cancer mass but also the stromal environment, allowing compartmentalization and the establishment of tumor-stromal borders.^[58] The compartmentalized co-cultures have allowed for the recreation of interstitial pressures with a high level of reproducibility. Both glucose and oxygen diffusion were found to be high, and there was adequate oxygen and nutrition permeability.^[46] However, endogenous tumor-associated stromal components, like immune cells and fibroblasts, have not been used in conventional organoid approaches.^[46,59]

Biological scaffold models like decellularized extracellular matrix (dECM), Matrigel, and collagen have been widely used to build ECM architectures able to recreate the natural environment for tumor cells. It is possible to co-culture with stromal cells and add chemical agents and proteins from the ECM.^[60] With 3D printing technology allowing the design of more complex models with well-defined structures and compositions in a very reproducible way, it has increased control over the spatial and temporal distribution of cells.^[13,61,62] Decellularization techniques, however, may change the original tissue's porosity and stiffness, which impacts cellular responses, but they also enable the co-culture of stromal cells, the incorporation of chemical agents, and the addition of ECM proteins.^[63] Nonetheless, whilst these models provide high throughput and generally have good nutrient and oxygen permeability, they can be costly.^[46,64] The engineering of 3D tumor models using 3D bioprinting involves the layer-by-layer deposition of bioinks such as tissue spheroids, cell pellets, microcarriers, dECM components, and cell-laden hydrogels, all spatially defined.^[65] As a result, the concentration, porosity, and stiffness of the model may be adjusted. But, in these engineered 3D tumor models, reduced cell survival and cell attachment may occur due to their artificial construction and the origin of the bioinks employed.^[66] Nonetheless, all these models strive to reproduce the complex architecture of tumors, their heterogeneity, migratory activity, or the influence of mechanical forces like shear stress or hydrostatic pressure.^[46]

Other drawbacks are the lack of vascularization and dynamic stimulation, which do not allow the reproduction of mechanical forces involved in tumor progression, incapacitating cells' progression to the full spectrum of phenotypes found in real tumors.^[67] Mechanical cues from the TME promote tumor growth, triggering mechanotransduction pathways that result in phenotypic modifications. It is well known that matrix stiffness and shear stress from fluid flow contribute to tumor progression and drug resistance.^[68,69] Tissue–tissue interfaces and complex spatiotemporal architectures of the ECM and vasculature, to mention some, are 3D features that make possible biomechanical stimuli, such as flow and cyclic strain, or biochemical stimuli to a precise region. 3D features like the ones aforementioned are impossible to model in a 2D setting or in conventional 3D models.

2.3. In Vivo Cancer Models

Animal models are the gold standard since they can emulate the whole organism's complexity. Of all the several animals that had

their genome sequenced, the mouse (a murine species) is the most used animal model in the study of carcinogenesis.^[70] Still, they do not share the human genome, anatomy, or physiology, and as such, their immunological and inflammatory responses may differ from those of humans.^[71] However, there are different types of murine models that are still used and developed for tumorigenesis and tumor progression studies. Implanting tumor cells into animal models has long been an experimental model for the study of cancer biology.^[72] Whether the injected cells are in the form of cancer cell suspensions or in the form of a slice of tumor from a patient. These are inserted into a specific site of the animal model, which determines the type of model.^[73] If the injected cells or tissues are delivered to the anatomic location from which the tumor was derived, they are called orthotopic models, whereas if they are inserted in an ectopic site, they are defined as heterotopic. Since heterotopic models are injected into the mouse flank, they are very controllable and do not require much surgical know-how.^[72] These different kinds of cancer models can rely on grafted tumors derived from cell lines or explants or from genetically engineered mouse models (GEMM) to intrinsically develop the disease on their own.^[74] In non-GEMM models, to prevent graft rejection, this approach generally requires immunodeficient mice unless animal tumor cells are injected into syngeneic hosts.^[72] Besides the injection of tumors, chemically induced models can also be produced by the ingestion of some types of foods, creating sporadic models. These types of models are extremely limited since only a fraction of the mice develops tumors, and with variable location, diffusion, and differentiation, having low and longer tumor development.^[70]

A patient-derived xenograft (PDX), which is a tumor created by implanting patient tumor cells from tumor excision or biopsy into immunodeficient mice, has been demonstrated to preserve the donor's histology and genetic profile through several passages. The donor tissue stroma is frequently replaced by murine architecture, and the fastest-growing clones tend to take over, resulting in a progressive loss of the heterogeneity of the initial transplants.^[72] PDX models have shown to be valuable for research on cancer metastasis and drug resistance, as well as pre-clinical testing and the identification of novel anticancer drug candidates.^[75]

GEMM can be applied to investigate human disease and possibly create new treatments. However, the models only provide data for the early stages of illness and have less evidence for the latter stages. The native process of metastasis is not replicated by GEMM models, which exhibit a lesser degree of dispersal and require more time to metastasize.^[70] Although animal models may be the best choice for drug development today, the drawbacks pointed out above, together with associated ethical problems and high costs, the need for specialized personnel, the lack of high throughput, and the fact that they are time-consuming, show the immediate need for alternatives.^[76,77]

2.4. Tumor-on-a-Chip (ToC) Models

ToC are microfluidic devices that aim at mimicking important features of a tumor's physiology. The architecture of these microfabricated devices mimics tumor microenvironments and accommodates cells and tissues in an in vivo-like manner.

Additionally, by modulating the ToC components and their properties, individually or in combination, this synthetic biological approach controls biophysical, biochemical, cellular, and tissue features, enabling insight into the human cancer pathophysiology in an organ-relevant context.^[50] They explore microfluidics to act as a supply and drain of nutrients, gases, and metabolites capable of spatiotemporal control and relevant physiological mechanical stimulation. More than often, laminar flow inside the micrometer-sized channels is used for the spatial control of materials or the definition of chemical and physical gradients. Natural and synthetic biomaterials are used as matrices to embed multiple cell types typically present in tumorous tissue. The physical and biochemical properties of the native ECM are reproduced by these biomaterials to support and sustain cell adhesion, growth, and proliferation.^[78]

In this last decade, ToC technology has been widely adopted by academia in relevant studies of cancer physiology, elucidating cancer biomechanisms or drug screening, as examples. The complexity of the ToC devices is increasing, and different types of function-specific devices are being developed.^[79] Several stages of tumor progression and aggressiveness are modeled in these micrometric devices, already integrating cell–cell, cell–tissue, and tissue–tissue interactions to understand and depict the tumor cascade. Biological stages of tumor development, in which cells increase in malignancy through progressive multi-step alterations,^[80,81] were already replicated using ToC technology, namely angiogenesis, tumor progression, expansion, invasion, and metastasis.^[50] Although ToC is in an earlier development stage, preliminary results show that they have a strong potential to become an effective human model to recreate patient-specific tumor models to tackle fundamental studies of the physical and physiological properties of tissue, diagnostic tools, and therapeutic planning.^[39,82] Being capable of generating personalized tissue profiles, ToC models allow for testing the effectiveness of various treatments and thus guiding patient-specific therapeutic decisions. Innovative and promising therapies like immunotherapy have been recently explored in a preclinical setting using ToC technology for recreating and predicting tumor responses in a dynamic manner, such as with immune checkpoint inhibitors and adoptive cell-based therapy.^[83,84]

The possibility of integrating microsensors and the transparent nature of the shell materials allow for on-chip biophysiochemical analysis and real-time imaging of tissues.^[85] Microfluidics enables the potential for analysis of biochemical, genetic, and metabolic activity online within the chips and with low volumes of samples and reagents. Micro actuators are integrated to produce localized biophysiochemical stimulation or even to divert the direction of the flow.^[86] In the laboratory, these devices were initially manufactured by means of microchip fabrication technology, mainly by photolithography and using poly(dimethylsiloxane) (PDMS).^[78] Nowadays, other techniques like additive manufacturing (e.g., 3D printing, SLA, binder jetting, bioprinting, etc.) or subtractive manufacturing (micro milling, xurography, laser cutting, etc.) are also used and integrated in ToC development.^[87] By combining and integrating different technologies in the production process, the limitations of one technique are solved by the next, consequently allowing for the development of more complex ToCs. However, current ToC is still simple systems, lacking the integration of multiple com-

ponents of the TME with complex spatiotemporal distribution to achieve realistic functional microtissues.^[88] Even though ToC devices are being developed at a fast rate, the engineering and fabrication aspects of these complex devices are still far from the vision of industrially manufactured ToC devices. **Table 2** presents a summary of some of the ToC devices developed in the last 5 years.

3. Biofabrication of Tumor Microenvironment (TME)

Engineering a biologically accurate tumor model means developing a system capable of replicating the components and monitoring all the interactions found in a TME (see Section 2). The scaffold/matrix is one of the most important components of the tumor biological model since it is the biological medium that will mimic the ECM and, as such, is the environment provider for cancer cells. The ideal scaffold would facilitate cell adhesion, proliferation, and differentiation, enabling cell–ECM and cell–cell interactions. To meet the requirements of TME, it must be biocompatible, biodegradable, and have architecture and mechanical properties consistent with the *in vivo* ECM.^[60,89]

Scaffolds can be produced from a series of natural and/or synthetic materials. Synthetic polymers like polyethylene glycol or poly(ϵ -caprolactone) have the advantage of having easily tuneable and modulated properties. However, their synthetic nature results in low bioactivity and can release by-products that may change the TME. Unlike these, natural polymers like collagen, gelatin, and alginate have good biocompatibility and inherent bioactivity.^[90] As an alternative, dECM is a biomaterial that recreates the natural microenvironment, providing the necessary ECM biological cues to cells. However, as a natural biomaterial, it lacks mechanical stability.^[90] The combination of natural and synthetic polymers is being studied to achieve materials with high biological activity and mechanical stability.^[91]

The definition of the biochemical composition and biophysical characteristics of the materials, such as topography, stiffness, molecular density, and tension, will determine how cells will respond, influencing the quality of the results obtained using the model.^[60] In TE, there are several manufacturing techniques to produce different types of scaffolds with different physicochemical features. From nanoscale dimensions like electrospinning, freeze-drying, or self-assembly to larger dimensions like 3D printing and molding. However, for most ToC devices, the scaffold/matrix is either injected into the microchannels/chambers,^[92,93] or cast.^[94,95] A hybrid fabrication method for the ToC matrix is expected to considerably improve the technology.

Another critical component of the biological model is the cells that will form the microtissues. Cells behave differently according to their source. Commercially obtainable cell lines are usually easier to culture and manage, though they do not always faithfully reproduce organ physiology and function due to the homogeneity of the cell population.^[96] Pluripotent stem cells and primary cell types could also be used. However, human primary cells may best suit ToC development and testing since they can be obtained from the patient and consequently be used to describe the patient-specific tumor.^[97] The heterogeneity of tumors supports this choice.^[98] On the other hand, primary cells need specific procedures to be obtained and maintained *in vitro*. In the case of

Table 2. Overview of biological factors considered in some of the reviewed ToC models.

Tumor organ	Application	Materials			Tumor cell density	Flow values	Ref.
		Cells	Co-culture	Coating material / ECM			
Lung tumor-on-a-chip	Tumor growth and morphology	Human lung adenocarcinoma cell line (A549)	Human AMMSCs	Collagen I	0.5×10^6 cells mL ⁻¹	Static	[113]
	Tumor growth and morphology	Human lung adenocarcinoma cell line (A549)	N/A	Agarose	0.5×10^6 cells mL ⁻¹	2.5 μ L min ⁻¹	[114]
Brain tumor-on-a-chip	Drug testing and development	Slice of human glioblastoma grown in mice	N/A	N/A	N/Ref	1 mL h ⁻¹	[115]
	Tumor chemotaxis and cancer treatment	Hepatoma cell line (HepG2) and astrocytoma cell (U87 line)	BMECS and astrocytes	Collagen I	1×10^6 cells mL ⁻¹	static	[93]
	Tumor growth and morphology	Brain tumor tissue	N/A	N/A	10–15 mg pieces (2 × 2 × 2 mm ³)	4 mL min ⁻¹	[116]
Colorectal tumor-on-a-chip	Angiogenesis, microvasculature, and lymphatics	Human glioblastoma cells (U87MG)	HUVECs and lung fibroblast	Spheroid – Matrigel Gel – Fibrinogen	5000 cells well ⁻¹	Static	[117]
	Angiogenesis, microvasculature, and lymphatics	patient-derived brain tumor neurosphere culture (GS5)	HUVECs	Fibrinogen	0.5×10^6 cell mL ⁻¹	Max flow rate – 3.21 mm s ⁻¹	[118]
	Angiogenesis, microvasculature, and lymphatics	CRC cell lines (CRC268, CRC663, CRC1180)	EC, Monocyte cells, and normal human lung fibroblasts	Fibrinogen	5×10^6 cell mL ⁻¹	Static	[119]
Breast tumor-on-a-chip	Cancer treatment and drug development	Human colon cancer cell line (HCT-116)	HCoMECs	Matrigel	10×10^6 cells mL ⁻¹	8 μ L h ⁻¹	[120]
	Angiogenesis, microvasculature, and lymphatics	Human breast cancer cells (MCF-7)	HUVECs	GelMA	Several	Velocity- 5×10^{-7} cm s ⁻¹	[95]
	Cancer invasion and metastasis	MDA-MB-231 cells	HUVEC	Matrigel	10^6 cells mL ⁻¹	N/Ref	[121]
	Angiogenesis, microvasculature, and lymphatics	MDA-MB-231 cells	N/A	Collagen I	$1 \times 1 \times 2$ mm ³ slices	N/Ref	[122]
	Tumor chemotaxis and cancer treatment	Human lung adenocarcinoma (Calu-3)	Primary human fibroblast (IMR-90 and C5120)	Matrigel	30 μ L with 5000 cells	Static	[123]
	Immune microenvironment	Human breast cancer cells (MCF-7)	NK-92 and HUVECs	Collagen I	1.5×10^6 cell mL ⁻¹	N/Ref	[124]
	Immune microenvironment	MDA-MB-231	HUVEC, monocytes, and MCF-10A	Collagen	4×10^6 cells mL ⁻¹	Static	[125]
	Immune microenvironment	BT474 cell line	HUVECs, adenocarcinoma, breast CAF and immune cells	Channels – fibronectin Matrix – Collagen I	1×10^6 cells mL ⁻¹	1 mL min ⁻¹	[126]
	Angiogenesis, microvasculature, and lymphatics	MDA-MB-231, MCF-10A and MCF-7	HUVECs, NHLF	Fibrinogen	2×10^6 cells mL ⁻¹	5.2 mmH ₂ O	[127]
	Extravasation	Tumor chemotaxis	Breast cancer (MX-1)	N/A	Modified collagen	5×10^6 cells mL ⁻¹	0.03 mL h ⁻¹

(Continued)

Table 2. (Continued).

Tumor organ	Application	Materials	Tumor cell density	Flow values	Ref.	
Renal tumor-on-a-chip	Angiogenesis, microvasculature, and lymphatics	clear Renal Cell Carcinoma	Normal-adjacent renal cortex	Collagen I	16.6 cells μL^{-1}	0.5 $\mu\text{L min}^{-1}$ [129]
Pancreatic tumor-on-a-chip	Microenvironment-on-a-chip	Pancreatic cancer cell line (PANC-1)	Pancreatic stellate cell line	Collagen I	N/Ref	N/Ref [130]
Ovarian tumor-on-a-chip	Cancer invasion and metastasis	Ovarian carcinoma (A2780)	HOMECS	Collagen I fibronectin	5×10^5 cells mL^{-1}	1 dyne cm^{-2} [92]
Skin tumor-on-a-chip	Immune microenvironment	Murine melanoma cell line (B16F10-ova)	N/A	Matrigel Collagen	10 μL with 10^5 cells mL^{-1}	2 dynes cm^{-2} [94]
Cervix tumor-on-a-chip	Tumor growth and morphology	HeLa cells	HUVECs and Human lung fibroblast	Fibrinogen	N/Ref	Static [131]
Soft tissue tumor-on-a-chip	Tumor chemotaxis and cancer treatment	STS cell lines (STS117 and STS93)	N/A	N/A	2×10^6 cells mL^{-1}	Static [86]

stem cells, some ethical and practical questions still arise.^[99] Despite their origin, the primary concern would be to make sure that all necessary cell media components and functioning cell types are present and scaled in appropriate ratios.^[49]

Independently of the type of cells used, the way microtissues are introduced into the microphysiological device also varies. Cells may be suspended in a medium and flowed into the device to adhere to walls or biomaterials, or they may be introduced into biomaterial solutions and plotted into specific positions.^[100] In other cases, they are first turned into spheroids or aggregates and then further mixed in biomaterial solutions or placed in spatially relevant locations. Sliced tissues from real tumors may additionally be seeded in biomaterials or placed in microfluidic chambers. Subsequently, mediums, factors, and genes, which are non-cellular entities, are added to the scaffold/matrix or flowed through microfluidic paths to nourish and stimulate the cells toward maturation.^[100] Factors and genes may not always be added since they can be directly produced by cells. However, they may be added to simulate a specific period in the tumor cascade.^[50]

Spheroids are often made from cancer cell lines. They can be grown with or without a scaffold. Scaffold-free techniques are frequently employed since they are quite easy, quick, and affordable to implement.^[79] Pellet culture, which includes centrifuging a cell solution to concentrate the cells, is the simplest scaffold-free method. Although it frequently produces large-diameter spheroids, the centrifugal force aids in the promotion of cell–cell attachment. The shear force from spinning, which can affect cell morphology and orientation but also modulate cell–cell or cell–surface binding kinetics, influences the fate of cells, as well as the challenge of producing spheroids on a large scale, are drawbacks to this technology.^[101] The hanging drop method includes pipetting a cell suspension onto a lid, which is then turned upside down, causing the cells to aggregate due to surface tension and gravity.^[102] The initial cell count is used to adjust the spheroid's size, and co-culturing can produce heterotypic spheroids.^[103] The liquid overlay is another simple technique where cell suspen-

sions are plated on low-adhesive surface plates or on plates covered with materials like agarose that prevent cell attachment to the surfaces.^[104]

Organoids are also usually made from adult stem cells, induced pluripotent stem cells, or stem cells from an embryo. Such organoids develop structures that need a scaffold to provide an ECM. Organoids made from embryonic stem cells are expanded initially, then differentiated later to reach a fully differentiated state. Depending on the kind of tissue, the construction of a complicated structure usually takes two to three months to achieve and requires the application of various growth factors. Furthermore, adult stem cell-derived organoids use readily differentiated cells from samples of biopsies or resections. Pluripotent stem cell-derived organoids are seen to better model organogenesis, whereas adult stem cell-derived organoids mimic epithelial tissue regeneration.^[105] Each of these systems has a unique use and can be complementary to other(s).

The air–liquid interface method is another technique that enables the propagation of organoids with both stromal and epithelial cells. In cell culture inserts, frequently employed in cell migration assays, the oxygen supply to the cells is significantly increased compared to a submerged organoid approach because here the cells are embedded in scaffold gels that are in direct contact with air on the upper surface of the porous membrane. Through diffusion into the porous membrane, cells absorb nutrients and growth elements from the medium supplied on the bottom surface. The air–liquid interface technique has the benefit of not only retaining the TME for long periods but also including stromal cells.^[106] Although organoids produced using the air–liquid interface approach may recreate the TME and contain stromal and epithelial components, they lack tissue–tissue interactions and mechanical cues.^[43] These restrictions may be overcome by culturing organoids using ToC technology. ToC model design ideas could be paired with organoid self-organization principles to create effective tumor models. Despite their basic differences, ToC and organoids are seen as complementary models.^[107]

Tumor models can also be produced by reseeding cells in the dECM. This dECM can have different matrix stiffness, components, and structures, all of which affect the TME. The modification of their properties can be achieved by altering the conditions of growth. For instance, Lv et al.^[63] produced dECM scaffolds with various stiffnesses using MDA-MB-231 cells with varying levels of lysyl oxidase expression. These scaffolds provide a 3D environment during recellularization for the assessment of cell viability and cisplatin resistance.

3D bioprinting has also been used to replicate the TME. It takes advantage of CAD software and equipment to print bioinks that can contain spheroids, dECM components, and cell-laden hydrogels in a spatially controlled layer-by-layer fashion.^[108] Multiple technologies, like extrusion-based, droplet-based, and light-based bioprinting, among others, can be implemented using this method.^[109] A major advantage of 3D bioprinting for the development of in vitro tumor models is that it allows the user to regulate the deposition of numerous biomaterials as well as cells and biomolecules in a predefined structure. In addition, the ability to integrate perfusable vascular networks and the high-throughput fabrication of tumor models make bioprinting an attractive choice.^[110] Using multiple materials in one bioprint can produce multiple patient-specific models. In a study by Yi et al., three different inks were used to print multiple models on a glass substrate.^[111] A silicon ink was printed to define the borders of the model. A second ink containing glioblastoma cells embedded in brain dECM and a third ink with the dECM and endothelial cells were printed in a compartmentalized cancer-stroma concentric ring structure that recapitulated the TME. The model replicated clinically reported patient-specific resistances to concurrent chemoradiation and temozolomide therapy and suggested that it could be utilized to identify drug combinations that were most effective in tumor treatment. Structures like organoids that incorporate patient samples and are produced in a core-shell manner to maintain genetic heterogeneity alongside stromal populations were also employed in 3D bioprinting.^[112]

ToC technology to produce tumor models and the monetization of the TME are further explained in Sections 4 and 5.

4. Design and Fabrication of a Tumor-on-a-Chip

4.1. Conventional Materials and Fabrication Methods

In research, the mainstream material used in the majority of the currently manufactured ToC devices is PDMS. This polymer is optically clear, flexible, biocompatible, and low-cost, with properties that are advantageous for soft lithography and cell culture, as well as allowing the easy monitoring of the TME.^[39] Glass slides^[132] and coverslips,^[133] Petri dishes,^[134] and polystyrene (PS) omnitrays^[135] have been used as ToC substrates for the ease of placement and visualization on the microscope. This substrate is the bottom surface of the channel, and when bonded to the casted PDMS layer, the microfluidic channels and chambers are complete.

Soft lithography techniques from the semiconductor industry have been used for a long time to develop prototypes with PDMS. In a simple way, the soft lithography process is resumed by spinning coating a substrate (e.g., Si-wafer or glass) with a photosensitive material, photoresist (PR), to define the height of the chan-

nel mold, exposing the PR to UV light through a photomask to define the structures in the mold, and using a solvent to dissolve the unpolymerized PR. This process defines the geometry of the mold. The PDMS is then cast on the mold, peeled, and bonded to another substrate^[136] that can be PDMS, glass, Si, etc.

The exposure of the desired areas to the resist is made by means of a photomask. The fabrication of the photomask which originated in the semiconductor industry uses a CAD design to be imprinted on a substrate through specialized photolithographic or e-beam tools.^[137] However, some research groups are minimizing the costs and the expertise needed by using high-resolution printers to print transparency photomasks. These masks are made of opaque regions on transparent polymer films. Both Erdogan et al.^[138] and Chen et al.^[139] printed masks at 20 000 dpi to produce a ToC with minimum geometric features of 150 μm . According to the literature, the resolution can be further enhanced to 8 μm using photo-plotters operating at 20 000 dpi.^[140] As is understandable, photolithography and micro-molding processes involve a panoply of parameters that need to be fine-tuned so that the fluidic paths and chambers have the desired dimensions, access points, and surface characteristics.

The mainstream technique used in ToC for the bonding of two polymer surfaces is oxygen plasma treatment. This very reactive treatment modifies the atomic surface of the polymers, making them receptive to generating new bonds. Leaving the treated substrates in contact for a certain amount of time will irreversibly bond them together. In some cases, annealing is done to reinforce these bonds. This treatment can also be used to make the walls of the device hydrophilic.^[141,142]

Another geometric attribute of the ToC device is the access to the fluidic paths, generally made through inlets and outlets. Depending on the type of flow input technique, their geometry varies. ToC devices use passive pumping,^[134,143] hydrostatic pressure-driven micro pumping,^[127] syringe pumps, and/or vacuum to generate flow.^[115] Biopsy punches,^[133] razor-sharp punches,^[144] or blunt needles^[145] are widely used to punch the hole in the position of the inlets and outlets before substrate bonding. That access allows pipetting and the connection of tubing to vacuum, flow generators, or reservoirs. In some cases, large-size punches are used so that the inlet can be used as a reservoir,^[133] in others, Pyrex cloning cylinders^[138] or bottomless plastic vials^[146] are glued to each inlet or outlet to control the flow by fluid pressure. A funnel-shaped inlet was designed by Song et al.^[142] to address cell clogging that is observed in conventional cylindrical shaped inlets formed with hole punchers. To glue these reservoirs or tubing together, uncured PDMS or epoxy glue is usually used.

Montanez-Sauri et al., taking advantage of passive pumping and the positioning of the inlets, fabricated a microfluidic device composed of an array of 192 microchannels in which the inlets and outlets were conformed to a standard 384-well plate.^[135] Using this device together with automated liquid handling provided the means to perform a high throughput culture of T47D breast carcinoma cells in monocultures and co-cultures with human mammary fibroblasts in separate compartments.

A rectangular, linear microchannel with one inlet and one outlet is the simplest geometry of a ToC device that can be fabricated. Depending on the application and on the function to

Table 3. Technologies used in the fabrication of the ToC models review in Table 2.

Tumor organ	Technologies	Ref.
Lung tumor-on-a-Chip	Soft lithography, Spheroids on matrix	[113]
	3D printed mold, Spheroid on matrix	[114]
Brain tumor-on-a-Chip	CO ₂ laser, Micromachining, Thermal press, Solvent welding, Tissue slice	[115]
	Soft lithography, Cells on matrix	[93]
	Glass etching, Tissue slice	[116]
	Injection molding, Spheroid on a chamber	[117]
Colorectal tumor-on-a-Chip	Soft lithography, Cells on matrix	[118]
	Soft lithography, Cells on matrix	[119]
	Soft lithography, Cells on matrix	[120]
Breast tumor-on-a-Chip	Soft lithography, 3D printing (co-axial), Cells on matrix	[95]
	Laser cut	[121]
	Poly(methyl methacrylate) (PMMA) milling, Tissue slices	[122]
	Soft lithography, Spheroids on matrix	[123]
	Soft lithography, Removing rod	[124]
	Soft lithography, Cells on matrix	[125]
	Soft lithography, Cells on matrix	[126]
	Soft lithography, Cells on matrix	[127]
	Soft lithography, Cells on matrix	[128]
	Cells on matrix	[129]
Renal tumor-on-a-Chip	Spheroids on matrix	[130]
Pancreatic tumor-on-a-Chip	Soft lithography, Cells on matrix	[92]
Ovarian tumor-on-a-Chip	Soft lithography, Cells on matrix	[94]
Skin tumor-on-a-Chip	Soft lithography, Spheroids on matrix	[131]
Cervix tumor-on-a-Chip	Micromachining, Spheroid on chamber	[86]

model, ToC devices with multiple adjacent channels, multiple inlets, different-shaped chambers, multiple layers, and circular cross sections have been developed through soft lithography. Although the material used in the laboratory remains PDMS due to established techniques and low cost, its absorption of small hydrophobic molecules and its diffusion of gases, which are advantages in some types of models, become a great drawback in drug toxicity and factor detection models. The adulteration of results that the material can promote, together with the difficulty of fabricating PDMS devices at an industrial scale is leading to the development of new alternative materials for ToC fabrication.^[147] In the following topics, new alternative materials and techniques will be presented and discussed for different features of a ToC device, both at laboratorial and industrial scales (Tables 3 and 4):

4.2. Channels

Rizvi et al. used a simple, inexpensive, and widely accessible ToC design that uses medical-grade double-sided adhesive film between a glass coverslip and a PMMA plate.^[148] The channels' shape was defined in a 254 μm-thick adhesive by laser-micromachining as well as the inlet and outlet in the PMMA covering plate. After sterilizing all the components with isopropyl alcohol and air drying them under sterile conditions, the glass coverslip with the micromachined adhesive was placed on an icepack

inside the laminar flow hood and Matrigel was spread on the channel surface. Next, a PMMA plate was placed on top to complete the channels. After using epoxy glue to seal the silicon tubing to the inlets and outlets and leaving it at room temperature for Matrigel gelation, the device was ready for epithelial ovarian cancer cell seeding. In this 24 × 40 mm ToC, they fabricated 3 independent 4 × 25 mm, 254 μm-thick channels to evaluate, characterize, and visualize the progression and epithelial–mesenchymal transition of ovarian cancer cells under different flow conditions. Other examples of this cost-effective and straightforward integration for microfluidic fabrication and cell growth on a ToC device can be found for other applications.^[149–151]

Sacrificial materials that liquify during the polymerization of the solution-containing cells are yet another simple way to define micrometer-sized fluidic paths. Wan et al. micromilled a PMMA plate and printed poly(vinyl siloxane) to make a counter master to define a PDMS mold.^[152] This PDMS mold was filled with gelatin through the microchannel inlet. The gelatin with the channel geometry was placed at the bottom of a reservoir, and a solution of collagen was cast until the top. By incubating the device at 37 °C the collagen polymerized and the gelatin liquefied. Using a micropipette, the gelatin was removed from the device, and a hollow microchannel with an inlet and outlet became successfully defined inside the collagen structure. In this vascular 3D ECM, motile breast cancer cells seeded into the collagen were observed migrating to the vascular structure when chemical stimulation was introduced.

Table 4. Overview of materials and designs considered in the ToC models reviewed in Table 2.

Tumor organ	Geometric features			Materials		Dimensions		Ref.
		Interface	Chip	Channels [μm]	Interface [μm]	Chambers [μm]		
Lung tumor-on-a-Chip	3 parallel channels separated by pillars	PDMS	PDMS	1000 ^(a) 200 ^(b)	Pillars—160 pitch	N/A	[113]	
	Several designs	N/A	PDMS	N/A	N/A	N/A	[114]	
	40-well plate with individual channels to the central culture area	PTFE	PMMA	300 ^(b)	Membrane pore—0.4	N/A	[115]	
Brain tumor-on-a-Chip	3 lateral channels and an overlapping channel over one of the extremities	PC and PDMS	PDMS	Top—2000 × 500 Side— 2000 × 300 Center— 900 × 100 190 ^(a) 70 ^(b)	Membrane pore—0.4 and pillars	N/A	[93]	
Colorectal tumor-on-a-Chip	Tissue chamber with microchannel flowing below	N/Ref	Glass	100 ^(b)	N/Ref	20 μL	[116]	
	2 chambers separated by an elevated spheroid-sized well	N/A	PS	100 ^(b)	N/A	830 ^(c)	[117]	
	One central cell-gel loading channel and two lateral medium flow channels	N/Ref	N/Ref	500 ^(a) 250 ^(b)	AIM Biotech commercial chip Triangular pillars—100 pitch	1300 ^(a) 250 ^(b)	[118]	
Breast tumor-on-a-Chip	3 adjacent chambers with feeding lines in the extremities	PDMS	PDMS	N/Ref	Semiairc pillars—30 pitch	Central – 400 × 100 Adjacent – 200 × 100	[119]	
	Central circular chamber with 2 flanking channels separated by pillars	N/Ref	PDMS	100 ^(a) 126 ^(b)	N/Ref	5000 ^(c) 126 ^(b)	[120]	
	2 bioprinted channels crossing a chamber	N/A	PDMS	500 ^(c)	N/A	4000 × 4000	[95]	
Breast tumor-on-a-Chip	Microchannel with 2 adjacent chambers separated by membranes	PE and terephthalate	PDMS	1200 ^(a) 500 ^(b)	Membrane pore—8	Trapezoidbase – 9300 top – 3400	[121]	
	Rectangular chamber with 2 channels crossing transversally on both ends	N/A	Collagen	N/Ref	N/A	4000 × 1600	[122]	
	1 central chamber and 2 parallel channels	PDMS	PDMS	400 ^(a) 200 ^(b)	Microchannels 20 × 20 × 100	900 ^(a) 200 ^(b)	[123]	
Breast tumor-on-a-Chip	Chamber with a transversal channel at one end	N/A	PDMS	340 ^(c)	N/A	N/Ref	[124]	
	4 parallel channels	PDMS	PDMS	800 ^(a) 100 ^(b)	Pillars—30 pitch	N/A	[125]	
	5 parallel microchannels	PDMS	PDMS	several	Pillars	N/A	[126]	
Breast tumor-on-a-Chip	3 lateral channels	PDMS	PDMS	1000 ^(a) 150 ^(b)	N/Ref	N/A	[127]	
	Central cell culture compartment flanked by 2 perfusion compartments	PDMS	PDMS	200 ^(a) 100 ^(b)	Elliptical pillars—20 pitch	N/A	[128]	

(Continued)

Table 4. (Continued).

Tumor organ	Geometric features	Materials	Chip	Channels [μm]	Dimensions	Ref.
		Interface			Interface [μm]	Chambers [μm]
Renal tumor-on-a-Chip	Central endothelial circular channel surrounded by a matrix	N/A	Nortis microphysiological devices	120 ^(c)	Nortis commercial chip	N/A [129]
Pancreatic tumor-on-a-Chip	Seven lateral channels. Tumor cells in the central channel, sandwiched by medium sandwiched by fibroblasts, and by medium again	PDMS	PDMS	1000 ^(a) 190 ^(b)	Trapezoidal pillars—135 pitch	N/A [130]
Ovarian tumor-on-a-Chip	2 ECM chambers flanking a tumor chamber with a vascular chamber below the tumor one	PDMS	PDMS	1000 ^(a) 100 ^(b)	Hexagonal pillars—100 pitch Membrane pore—8	N/A [92]
Skin tumor-on-a-Chip	Tumor cells are covered by a membrane with an EC monolayer over which the microfluidic channel passes.	PC	PDMS	2000 ^(a) 200 ^(b)	Membrane pore—8	N/A [94]
Cervix tumor-on-a-Chip	1 central chamber and 2 parallel channels	PDMS	PDMS	1000 ^(a) 150 ^(b)	Pillars—100 pitch	1300 ^(a) 150 ^(b) [131]
Soft tissue tumor-on-a-Chip	4 parallel semi-circular channels, each containing 4 culture chambers connected in series	PDMS	PDMS	1000 ^(c)	Valves	21 wells in 500 × 500 × 500 [86]

^(a)width; ^(b)thickness; ^(c)diameter.

3D printing was also extensively used to fabricate microfluidics. It includes a fresh technique to print a removable sacrificial material,^[153] printing masters for casting,^[114,154] directly bioprinting the tissues onto a substrate,^[111] coaxially extruding materials to fabricate hollow perfused microchannels^[95] or printing the structure of the device.^[155] Another way to produce channels is by using direct-write laser micromachining in a substrate. Carbon dioxide (CO₂) lasers are often used to directly engrave channels into PMMA substrates^[156] or to cut parts to fabricate masters^[121] or devices.^[115] Micromilling^[86] and wet etching^[116] are also explored to directly engrave channels and other fluidic parts onto substrates.

4.3. Interfaces

Interfaces between adjacent channels are essential to properly mimic the borders between different tissues and, thus, the various biological barriers within the TME. ToC devices reviewed in Table 4 typically contain micropillars, microgrooves, guides, microchannels, or membranes between adjacent channels to sustain ECM-mimicking biomaterials or cell cultures and to establish the border (Figure 6). These interfaces usually serve to spatially control gradients of nutrients and oxygen, biochemical factors, or drugs within the system. Micropillars are placed in a periodic way along the limits of the adjacent channels. Dimensions, distances, and surface characteristics determine the profile of the interface. The contact area defined by the interface will influence the diffusion of (bio)chemicals and the shear stress caused by the flowing medium.

The pitch and shape of the micropillars vary in the literature.^[92,118,128] The formats and pitches must be designed according to the material used since the surface tension of the material will be the feature that holds the biomaterials (e.g., hydrogels) in the desired positions. An example can be found in Kim et al.,^[133] in which the authors use different micropillars to achieve multiple interfaces on the same chip.

Another way of implementing interfaces is by using membranes with micropores. Although it requires more fabrication steps, it is an efficient way of hindering the passage of unwanted material to cross the interface. Polyester,^[142] polycarbonate (PC),^[93] polyethylene terephthalate,^[121] and PDMS^[145,157] membranes are commercially available or can be fabricated in-house and can have pores ranging from hundreds of nanometers to a few micrometers. They are typically used to promote flow between channels that overlap or are laterally adjacent.^[121]

Another way to use surface tension to support and guide the flow and cells is to produce small continuous structures between channels that will pin the biomaterial meniscus.^[117] These so-called phase guides were already explored in ToC architecture.^[158,159] and are commercialized in chip arrays with various formats. These interfaces can also be created by smaller microchannels perpendicular to the main channels,^[160] by removing rods^[161] or sacrificial materials^[162] inside a biomaterial structure.

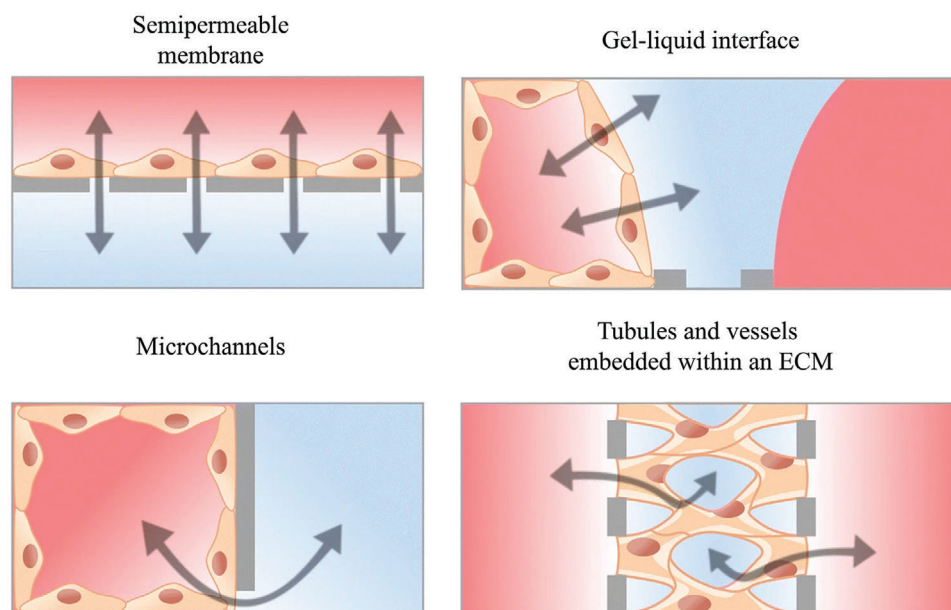


Figure 6. Different types of interfaces. Flow (blue)/Biomaterial (red). Adapted under the terms of the CC-BY Creative Commons Attribution 4.0 International license (<https://creativecommons.org/licenses/by/4.0>).^[163] Copyright 2021, The Authors, published by BMC, part of Springer Nature.

4.4. Actuators

Actuators are used in ToC devices mainly to alter or induce mechanical stresses in tissues, either by directly applying a force to the tissue or by altering the flow paths or profiles. Peristaltic pumps, syringe pumps, or other instruments imposing a pressure drop between the fluidic inlets and outlets are the most commonly used actuators to induce a given shear stress in the tissues, which consequently alters the TME.^[68,69] The “lung on a chip” integrates actuation to simulate the rhythmic respiratory movements of lungs and to create an *in vitro* human orthotopic model of a lung tumor.^[164] It is composed of two overlapped channels separated by a porous membrane. These two channels are laterally sandwiched between vacuum chambers that, when the vac-

uum is applied, force the membrane and the cells seeded on it to stretch (**Figure 7**). This strategy additionally served to study the stretching effect in fibroblasts and compare both CAF and normal tissue-associated fibroblasts (NAF).^[145] The results indicated that the phenotypes of stretched NAF are comparable to those of CAF, suggesting that mechanical stress is a key element in NAF activation and CAF generation. This same design was also applied to produce gut-on-a-chip devices.^[165] In this case, the mechanical deformations generated by the vacuum chambers simulate the cyclic peristaltic movements of the gut.

In some cases, valves are used to provide spatiotemporal control over fluid release and diffusion. For example, Hsu et al. cultured tumor cells and fibroblasts in two chambers separated

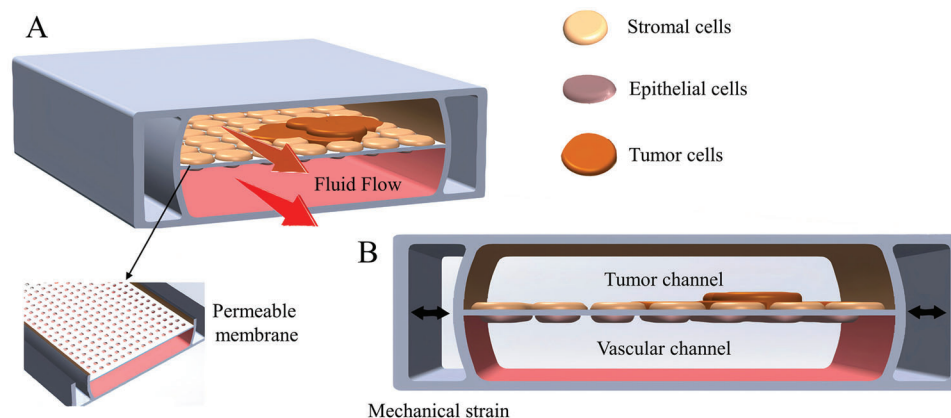


Figure 7. A) Schematic of a lung ToC containing a vascular channel and a tumor tissue channel separated by a porous membrane and 2 lateral vacuum chambers for mechanical stimulation. Isometric view. B) Frontal view.

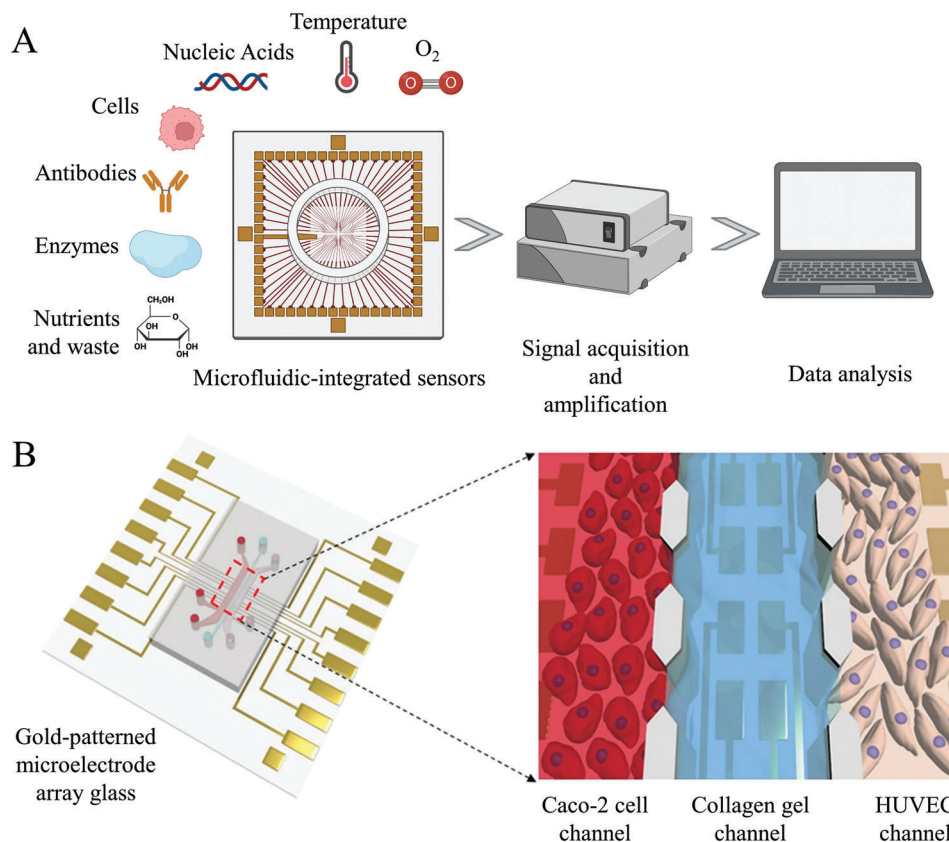


Figure 8. A) Schematic illustration of the data acquisition steps. Created using Biorender.com. B) Schematic of a gut-on-a-chip. The left channel was used to establish an intestinal lumen using human epithelial Caco-2 cells. The right channel was employed to make a vascular lumen using HUVECs. B) Adapted under the terms of the CC-BY Creative Commons Attribution 4.0 International license (<https://creativecommons.org/licenses/by/4.0>).^[182] Copyright 2022, The Authors, published by Springer Nature.

by a valve.^[156] When the vacuum was applied to the valve chambers in the bottom layer, the thin middle layer of PDMS deflected and allowed medium in the cell culture chambers in the top layer to flow between both. This strategy allowed the analysis of the paracrine loop between both cultures. Rerouting of fluid between the three chambers was also implemented for the study of interactions among lung cancer cells, macrophages, and myofibroblasts.^[166] The use of magnet force is also used to block the flow by acting on a metal rod to push a PDMS layer into a channel.^[86] Another strategy focuses on the use of pneumatic valves to control the flow between the four chambers. Feng et al. used 3D printed masters and added superparamagnetic iron oxide nanoparticles (NP) to the PDMS-casted chambers to perform magnetic hyperthermia treatment by facilitating NP penetration in ECM biomaterial. Even though the actuator is off-chip, the control of heat fluxes through this technique affects the tumor spheroid at the nanoscale, which, in conjunction with valves and flow, can impose the temperature of the system.^[167] Another example of external actuation implemented in ToC technology is X-ray. The exposure of a microfluidic device containing soft tissue sarcoma spheroids to multiple X-ray radiation doses was performed by Bavoux et al. to study the influence of a synergetic treatment both with pharmaceutical compounds (Talazoparib, Pazopanib, AZD7762) and radiotherapy.^[86]

4.5. Sensors

To achieve high-throughput physiological data collecting, the so-called smart ToC devices must accurately monitor the biochemical and biophysical parameters of the TME and, in the future, provide data for analysis using artificial intelligence.^[168] Biosensors integration in ToC devices must be capable of measuring physiobiochemical markers of the metabolic and functional status of cells and their response to specific stimuli. Integrating on-chip analysis methods to assess tumor model viability and mimicry is the next step in complex ToC design (Figure 8). Physical and electrochemical sensors to measure, for example, pH,^[169] oxygen,^[170] temperature,^[171] impedance^[172,173] or glucose and lactate levels^[174,175] are already being integrated into extremely simple models like hanging drops^[174] or spheroids in wells.^[176] Arrays of sensors or sensor modules could be particularly efficient for automated capabilities and for real-time monitoring of multiple physical or (bio)chemical signals in a non-invasive manner.^[177,178] This implementation is seen as a useful alternative for the analysis of cross-ToC interactions or even intra-ToC flow-related parameters. Nonetheless, the measurement of physiochemical parameters in a precise spatiotemporal location in the near vicinities of the tumorigenic tissue poses enormous challenges.

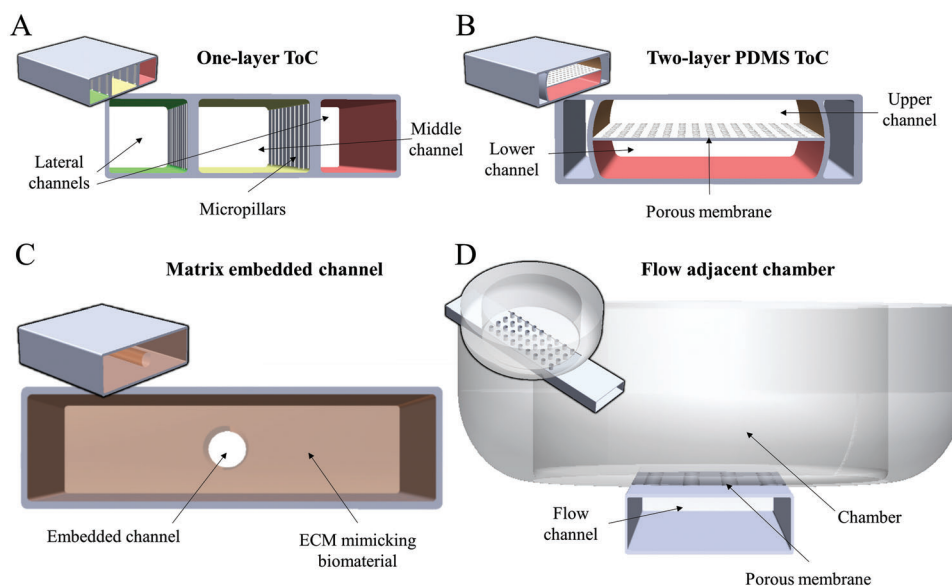


Figure 9. Schematic representation of the different ToC designs. A) One-layer ToC with 3 lateral channels. B) Two-layer PDMS ToC with 2 channels separated by a permeable membrane. C) ToC with a matrix-embedded channel. D) A chamber over a fluidic channel for exchange between the tissue and the flow.

So far, macro imaging techniques are the mainstream assessment tools used with ToC devices. The transparent nature of the devices and their size enable flow and tissue observation under microscopes. Commonly used microscopy and fluorescence techniques often require specialized personal and expensive equipment, and, in many cases, the destruction of the tissue is necessary for evaluation. More recently, efforts have been made to integrate on-chip low-cost, and automated imaging.^[179,180] Moreover, computational tools like machine learning and artificial intelligence are being applied to data analysis of these types of devices.^[168,181]

5. Recent Architectures of ToC Models

ToC devices have been an area of extensive study. The first microfluidic device capable of separating and measuring individual events of the metastasis process was developed in 2007.^[183] Since then, several tumor-specific functions have been mimicked on these microfluidic devices, with multiple features, different tumor types, and co-cultures. According to our classification, ToC architectures can be classified into four major groups: one-layer ToC, Two-layer PDMS ToC, matrix-embedded channel, and flow-adjacent chamber (Figure 9).

5.1. One-Layer Straight Channels

One of the simplest designs in ToC devices consists of linear adjacent channels, each containing a different cell type, a co-culture of different cell types, or simply working as a fluidic passage (Figure 9A). Different tumor functions are commonly addressed using this design and approach.^[113,123] The most used material to fabricate these systems in the Lab is still PDMS through soft-lithography, but other materials and techniques are being pursued to implement the fabrication at a larger scale. The flow in

these systems can be controlled in different manners, for example, by hydrostatic pressure, positive pressure, negative pressure, capillary forces, gradients, etc.

An example of a successful PDMS system with 3 adjacent rectangular cross section channels being used to replicate tumor progression at early stages (Figure 10), was seeded with

HeLa/fibroblast spheroids and epithelial cells (EC) in a fibrinogen solution in the middle channel while a solution of endothelial cell medium flows through both lateral channels. With this simple design, the authors were able to study tumor behavior under the influence of ECs and fibroblasts.^[131] A similar design seeded MX-1 cells in a modified collagen solution (middle channel) and filled with a chemoattractant-containing medium (lateral channels) achieved a biologically relevant 3D environment to resolve different aspects of cancer intravasation.^[128]

Another microfluidic device with 3 linear adjacent PDMS channels with rectangular cross section (available in the market) was used to evaluate the dynamics of ex vivo brain tumor stem-like cells.^[118] The system employed to develop a perivascular niche model was seeded with a co-culture of patient-derived brain tumor neurospheres, GS5 combined with human umbilical vein endothelial cells (HUVECs) in a fibrinogen solution (middle channel). An analogous design was applied to simulate tumor cell extravasation.^[121] This was fabricated by laser cutting a PMMA plate master to cast the PDMS mold, resulting in a faster, cheaper, and easier solution compared to photolithography. AIM Biotech is one of the companies providing this design, incorporating multiple chips per plate of PC. Instead of soft lithography and PDMS, these plates are fabricated by injection molding for a faster and more cost-effective process. In this case, the resolution of channel dimensions will depend on the capabilities for the fabrication of the master in a metallic substrate. Techniques, such as micromilling or laser sintering, are suitable candidates for this fabrication.

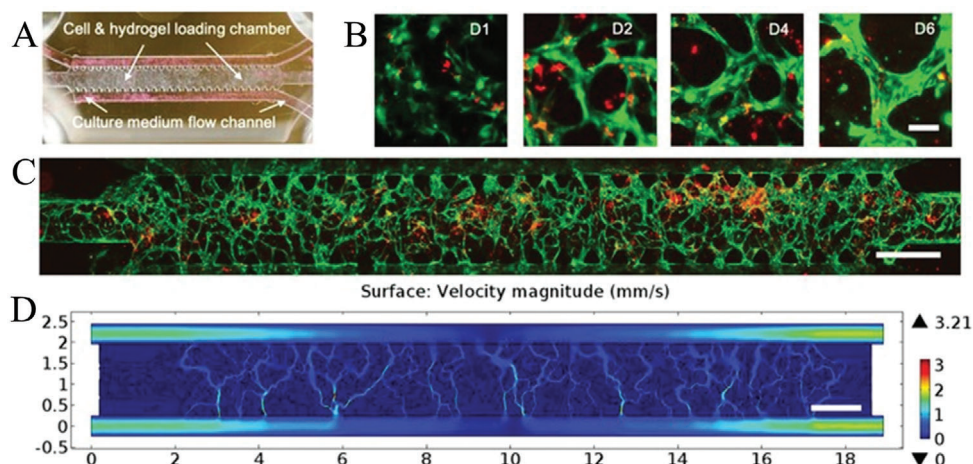


Figure 10. Example of three adjacent straight channels in one-layer fabricated by AIM Biotech and used by Xiao et al. for the growth of brain tumor stem-like cell-incorporated microvasculature-on-a-chip. Microfluidic device ($250\ \mu\text{m}$ in height) containing a cell/gel loading micro-chamber ($8000\ \mu\text{m} \times 1300\ \mu\text{m}$) flanked by two medium flow channels ($500\ \mu\text{m}$ in width). An array of triangular microposts separate the gel chamber and the medium flow channel, allowing for loading and confining the hydrogel precursor to the mid chamber only. Scale bar: $1000\ \mu\text{m}$. A) Representative time course images of the microvessel formation over a period of 6 days. Scale bar: $15\ \mu\text{m}$. Green: GFP-HUVEC. B) Whole chip scan showing microvasculature formation (96 h postcell in fibrin) and loading of single BTSCs (GS5). Green: GFP-HUVECs. Red: BTSCs. Scale bar: $1000\ \mu\text{m}$. C) Comsol Finite Element Simulation of flow velocity magnitude (mm s^{-1}). The finite element model was constructed using the experimental whole-chip microvessel network in (C). A–D) Adapted under the terms of the CC-BY Creative Commons Attribution 4.0 International license (<https://creativecommons.org/licenses/by/4.0>).^[118] Copyright 2019, The Authors, published by Wiley-VCH.

The design of the channels usually has a rectangular cross section, but other geometries are also possible. For example, a middle channel can have a circular shape enclosing colorectal tumor cells in Matrigel solution and two adjacent channels seeded with human colonic microvascular endothelial cells (HCoMECs) to assess the dose-response effect of cells.^[120] In this study, gemcitabine was delivered through drug-loaded CMChT/PAMAM nanoparticle gradients, both with spheroids and/or cell culture.

Designs with more than three straight rectangular cross section adjacent channels are also common. Mi et al.^[125] studied tumor-macrophage bidirectional crosstalk in a 4-channel device with the medium flow (lateral channels) and tumor and non-tumor cells (middle channels). Another example is given by Nguyen et al. where the authors studied the effects of the delivery of trastuzumab drug to the tumor.^[126] The authors used a 5-channel device in the combination: middle channel seeded with HUVECs simulating vascularization; lateral channels adjacent to the middle seeded with a co-culture of HER2 breast cancer, CAF, and immune cells; and the two most lateral channels serving as medium reservoirs. The design was also tested with seven adjacent channels.^[119,130]

Tissues are influenced by interfaces in all directions of the 3D space. One-layer straight channels allow for paired interfaces, always communicating laterally with one another. This arrangement limits the movement of cells and gradients, meaning they do not represent a real 3D environment.

5.2. Two-Layer PDMS ToC

This arrangement can be seen as the stacking of two one-layered ToC, separated by a permeable membrane (Figure 9B). In particular, a simple three-linear adjacent upper channel configura-

tion can communicate with a one-linear lower channel through a micrometer-sized pore PDMS membrane.^[92] This design enabled the observation of extravasation of cells from the lower channel to the central upper channel with the tumor, and to study the effect on triggering tumor migration to the ECM. Inverted designs were implemented by imposing the interface through the membrane only from the lateral lower channel (of three) to the one-linear upper channel. Hepatic drug metabolism in glioblastoma was addressed with this architecture.^[93] The lower left channel, connected to the upper channel through a PC membrane, contained brain microvascular endothelial cells (BMECs) and astrocytes. The lower central channel enclosed a collagen solution and the lower right channel U87 glioblastoma cells. The drugs were introduced in the upper channel to simulate hepatic metabolism and the effects of blood–brain barrier penetration.

Other simplistic designs consisted of molding one-linear PDMS channels resorting to two micromilled PMMA plates.^[94] The one-linear channels were separated by a micrometer-size pore PC membrane to study the infiltration of T cells into the tumor tissue. Emulate, Inc. is commercializing this design in PDMS. Studies performed on their chips can be found elsewhere.^[184]

The two-layer ToC is the reference for mechanical stimulation and allows an increase in the number of possible interfaces, both laterally and vertically. Despite multiple interfaces effectively improve control of the spatiotemporal location of each culture, this architecture still does not provide an effective 3D environment.

5.3. Matrix-Embedded Channels

An alternative way to fabricate ToC is to pour biomaterials that mimic ECM over channels made from sacrificial or permanent

molds. In this type of design, cell cultures are part of the structure of the channels instead of being seeded inside them (Figure 9C).

A simple design of this type of ToC was demonstrated by Ayuso et al.,^[124,162] to evaluate natural killer (NK) cell response. The authors used soft-lithography to produce PDMS structures (chamber and rod). A solution of collagen with MCF7 cells and NK-92 immune cells was injected into the chamber and polymerized.^[124] The rod served as a master to mold the hydrogel and is removed after polymerization. This resulted in a transversal channel that was seeded with HUVECs, successfully demonstrating how natural killer cells respond to a tumor-induced suppressive environment. The latter allowed the removal of cell-laden hydrogel from the device for further evaluation.

In another approach, a main chamber is superimposed by rigorously placed sacrificial templates to define channels. This tumor model was explored to evaluate the diffusion of various drugs through the TME^[122] or to evaluate tumor cell migration in different fetal bovine serum concentrations.^[152] The design consists of a laser-cut PMMA plate as a rectangular chamber, and two gelatine sacrificial templates placed at each end of the chamber to define the microchannels. Tumor fragments are equally spaced between the templates. The chamber is filled with a collagen solution, which is crosslinked. The gelatin is then dissolved to form hollow channels.

Bioprinting is an alternative fabrication technique to define microchannels that can mimic vascular and lymphatic vessels by means of a three-needle co-axial nozzle. For example, the diffusion of drugs and biomolecules in the TME was mimicked using a ToC capable of reproducing both delivery and drainage routes of the vascular system.^[95] In this device, a PDMS chamber was half-filled with GelMA containing MCF-7 tumor cells. Two bioprinted microvessels were horizontally placed at the chamber half-height. Another layer of GelMA filled the remaining chamber. Polymerization followed. HUVECs were seeded in an open microvessel while HLECs were implanted in an end-blinded microvessel.

Nortis commercializes disposable microfluidic chips with this design, in which one channel branches or goes to a chamber and is used to inject the ECM biomaterial loaded with cells. A channel perpendicular to the first has a glass mandrel that crosses the biomaterial. After polymerization, the mandrel is removed, and a perfusable microchannel becomes available. Miller et al.^[129] used this commercial chip to develop the first vascularized, microphysiological biomimetic microfluidic device. The authors studied primary human clear renal cell carcinoma that retained the tumor's key angiogenic characteristics.

Unlike one-layer straight channels, matrix-embedded channels increase the directions in which cells and molecules can propagate and diffuse. The absence of pillars and the presence of ECM mimicking material in all directions of the fluidic channel better reproduce the *in vivo* conditions.

5.4. Flow-Adjacent Chamber

Flow-adjacent chamber architectures include a chamber suspended over the fluidic microchannel (Figure 9D). One example uses two glass layers thermally bonded to maintain human glioblastoma tissue *ex vivo* for long periods.^[116] The bottom Y-shaped channel was wet etched while the chamber, inlets, and

outlets, on top, were drilled. A semipermeable barrier was placed in between to avoid the permeation of cells, inhibiting clogging of the channel. The chamber was then pressure-sealed with a polyetheretherketone micropore. A 2 mm³ glioblastoma (GBM) tissue was injected into the chamber, and the channel was perfused with media. Another design, aiming at developing an easy-to-use, scalable, and reproducible ToC was made by injection molding of PS following a standardized 96-well plate format capable of holding 48 ToC.^[117] The ToC is comprised of a central chamber defined on an elevated rail guide. GBM spheroids were deposited onto lung fibroblasts in a fibrin gel, already injected in the chamber, to investigate tumor-related angiogenesis. For this, the authors additionally seeded HUVECs in medium on each side of the elevated rail. Models for vasculogenesis, tumor migration, angiogenesis, and tumor angiogenesis were achieved with this architecture.

Thermoplastics other than PS favorable to study tumors are poly(tetrafluoroethylene) (PTFE) and PMMA. A ToC design based on the prior premises was patented for multiplex drug testing in live tissue culture.^[115] It consists of a network of 40 channels feeding a clinical sample of tumor tissue in a side-by-side manner for the assessment of apoptosis and proliferation of the tumor. The plain bottom sheet (sealing layer) seals an intermediate micrometer-thick sheet that defines laser-cut channels (channel layer). The top layer (bottomless 40 well-plate) consists of 40 micromachined bottomless wells connecting each to the 40 microchannels below. The top layer additionally has a central area for tissue placement. A PTFE porous membrane was placed between the channel layer and the top layer, in the central region, to permeate fluid to the tissue. Solvent bonding and thermal pressing were used to adhere to the three PMMA parts. A slice of the live tumor biopsy is placed on the porous membrane. Negative pressure is imposed at one outlet to promote the medium containing the drug to diffuse to the tissue slice in a parallel fashion.

The flow-adjacent design is already commercialized by React4life and has been applied for various tumor studies.^[185]

This type of design allows the use of larger tumor tissue or cellular samples, expediting the use of clinical samples and mm-size tissues.

5.5. Multiple or Integrated Architectures Designs

The ToC designs described previously are grouped according to typical design features. But, even though a great number of unique designs exist, they are frequently a combination of primary features and architectures reported above. As an example, Chi et al.^[186] used a device that has a flow-adjacent chamber design (Section 5.4) combined with multiple chambers connected in series (Section 5.1). In order to simulate specific tumor-stroma complexity and tumor-endothelium interactions, the study incorporates tumor microvasculature and tumor-stromal microenvironment, including breast cancer invasion through the leaky microvasculature and angiogenesis. Another work shows combined elements in which a two-layer PDMS design (Section 5.2) uses micropillars to trap spheroids in the desired place (Section 5.1).^[187] This design simulates two important biological barriers to explore NP extravasation across leaky vasculature and its subsequent accumulation in tumor tissues: tumor leaky

vasculature and 3D tumor tissue with rich ECM. In another example, the authors fabricated a bottom layer composed of wells in a hydrogel substrate (Section 5.4) pressed onto a microfluidic channel 3D printed on a porous membrane assisted by sacrificial material (Section 5.3).^[188] The device was then sealed by pressing both layers together with the help of disk magnets and put to use to observe the interactional dynamics of neutrophils and growing tumor aggregates. In this study, the team observed that neutrophils respond to the growing tumor spheroids through both chemotaxis and the generation of neutrophil extracellular traps.

The combination of architectures in one chip or the connection between chips allows for connecting various models or various organs. For example, the reproduction of metastasis can be simulated by connecting models that simulate extravasation and intravasation. A ToC with multiple organ models or the connection of a ToC to other organs-on-chip allows us to see how metastasis sites would form on those tissues.^[189] This assembly is also useful for drug testing. The resulting data would infer the effects not only on the tumorigenic tissues but also on the other organ systems.^[190] The literature presents an ever-wider variety of designs, materials, and fabrication techniques (Table 4). An example of a design not included in the previous subsections consists of a well array in the bottom layer seeded with spheroids and an array of antibody-coated microarrays in the top layer. When closed together, the ToC enabled the study of interactions between antibodies and T cells with the tumor spheroids,^[191] as well as the co-culture of hepatocytes with tumor cells.^[192] The simplicity of another design, comprised of a chamber with arrays of pillars made use of hand-cut tape as a PDMS master for its photolithographic-free fabrication, developing a simple model for tumor metastasis. Moreover, CTC detection and isolation make use of specific architectures that are sometimes referred to as ToCs, even if they are more complex than the designs reported earlier. Usually for this end, the microfluidic ToC devices integrate several features such as mixing, separation, focusing, trapping, etc., described elsewhere.^[193,194]

6. Conclusions and Future Perspectives

ToC interest has been increasing over the last decade and is becoming a field of extreme multidisciplinary. Biologists, geneticists, chemists, and engineers are working together to understand the biological aspects behind tumor origin and cascade while, at the same time, testing therapies and drugs by developing the ToC using well-established technologies for microfluidics fabrication. This straightforward use of microfluidics techniques has resulted relatively well-developed proof-of-concept for ToC technology, but without a clear reference to the properties, geometries, actuation, and sensing optimization used, together with biomaterials and cell culture features, its full potential will take even longer to be achieved. This lack of information is perhaps one of the main setbacks for the development and use of microfluidic ToC technology, leading more than often to unreproducible results. Moreover, a large quantity of published work with related tissues and functions, in which the dimensions, flow conditions, biomaterials features, etc., are not characterized or

presented in units that can be related to each other, makes it extremely difficult to intercompare.

Since the initial development of new ToC systems often relies on complex microfabrication techniques and structures, it is crucial to investigate the design for accurate control of the physicochemical parameters in the device. Furthermore, not all researchers or users have a strong understanding of available microfabrication tools and their strengths and limitations for the development of ToC. It becomes essential to create user-friendly systems with standardized features and protocols for faster adoption, industrialization, and clinical translation.

The development of both microfabrication techniques and microfluidics has significantly increased in the last decades, but the lack of sensing and actuation elements on the ToC demonstrates that these advances are not being fully implemented in this field. Combining micro/nano-fabrication tools, microfluidics, TE, 3D bioprinting, and the panoply of additive and subtractive manufacturing techniques is probably the best way to produce differentiated models with high spatiotemporal control and resolution of the TME components. Advanced modeling techniques with innovative biomaterials, long-term culture, the individual context of cellular and non-cellular components, TE strategies, and manufacturing techniques will all be important for the consistency of ToC development and use. Other important features are automation and the connections of the ToC to the world, that is, the development of standard plug-and-play from the ToC to existing apparatus and analytical tools for automated medium changes, chemical additions, fluid flow regulation, or real-time measurements of tissue condition, as examples, have the potential to improve consistency and the number of tissues that can be grown. Moreover, materials engineering and characterization will be needed both for the exploitation of new biocompatible materials to serve as structures in these devices as well as bioactive materials for improved tissue culture.

Nowadays, projected devices are made for high-throughput with simplistic models, better suited for drug testing and development, tissue–tissue interaction studies, or to develop new immune, radio, chemo, and cell therapies. To clearly evaluate the factors that influence the heterogeneity inherent to the tumor, the model must contain the tumor and stromal networks found in *in vivo* tumors. But the physiological structure and TME *in vivo*, such as the reproduction of complex signals and the functions and responses of non-adjacent organs like the endocrine and immune systems, are intricate and not yet fully understood.

To date, companies that mass produce and sell microfluidic devices for tissue culturing, provide simple products fabricated by injection molding in a well-characterized inert polymer and, in some cases, pre-seeding them with commercial cell lines in a matrix of the most commonly used biomaterials. Although some ToC devices for laboratory use are available on the market, they often lack the necessary complexity and reproducibility for use in cancer research. But for fast, ready, and easy-to-use models for precise medicine, the ToC device must be precultured with appropriate TME components to only receive the patient-derived tumor cells for culture and testing.

The development and widespread use of microfluidic ToC technology face a variety of challenges:

Technical challenges

- Multidisciplinary teams
- Standardization of units
- Lack of elements to reproduce results
- Utilization of materials and techniques at the lab scale is challenging to translate for industrial manufacturing

Technological challenges

- Microfabrication techniques integration
- Sensing and actuation integration
- Integration with already existing analytical equipment
- Plug and play with existing flow control equipment
- Integration with multiple organ-on-a-chip

Biological challenges

- Mimic tumor real 3D architecture
- Vascularization spatiotemporal location
- Gradients of nutrients and metabolites
- Multicellular cultures
- Trustworthy clinical representation and translation
- Multiple biological systems

While ToC technology has the potential to revolutionize cancer research, these significant challenges prevent its translation to the industrial scale. Although promising platforms to produce patient-specific models of tumors, ToC are still in their early stages of development, and far more complex models must be created to reproduce in vivo tumor heterogeneity, processes, and the full microenvironment. Multi-model devices, such as human-on-a-chip devices, are seen as promising to achieve these goals.

ToC technology already provides various advantages in cancer research, including faster and real-time results, precise and targeted studies, the ability to mimic interactions between different cell types and biological structures, and the impact of physical and mechanical stresses on tumor growth. Moreover, ToC models have the potential for high throughput and scalability, as well as application in personalized medicine and drug discovery. Furthermore, ToC models were seen to successfully substitute animal models, reducing the number of animals used in experiments, which is consistent with the 3 R policy objectives.

This review points out that well-integrated microfluidic ToC devices and know-how have the potential to uncover the most intricate secrets of tumor biology and to stretch the knowledge about their invasiveness potential to other organs as well as to establish realistic predictive therapeutic models.

Acknowledgements

This work was supported by the Fundação para a Ciência e a Tecnologia (FCT) and Centro2020 through UIDP/04044/2020 and PAMI – ROTEIRO/0328/2013 (N° 022158) and by the FCT/MCTES (PIDDAC) through Associate Laboratory ARISE LA/P/0112/2020. G.G. thanks to the FCT for the Programme Stimulus of Scientific Employment – Individual Support (CEECIND/01913/2017) and financial support of project CARBONCT (2022.03596.PTDC). The financial support of TEMA is also acknowledged by the projects UIDB/00481/2020 and UIDP/00481/2020 from FCT and CENTRO-01-0145-FEDER-022083—Centro Portugal Regional Operational Programme (Centro 2020), under the PORTUGAL

2020 Partnership Agreement, through the European Regional Development Fund. V.S. would like to acknowledge the FCT, I.P., for funding of the Research Unit INESC MN (UID/05367/2020) through pluriannual BASE and PROGRAMATICO and project LA/P/0140/2020 of the Associate Laboratory Institute for Health and Bioeconomy – i4HB. This project (20NRM02 MFMET) has received funding from the EMPIR programme co-financed by the Participating States and from the European Union's Horizon 2020 research and innovation programme. J.F.G. thanks FCT for the PhD grant UI/BD/151259/2021. C.S.M. thanks the National funding by FCT, P.I., through the institutional scientific employment program-contract (CEECINST/00077/2021). H.A.S. acknowledges financial support from the Academy of Finland (Decision no. 331151) and the UMCG Research Funds.

Conflict of Interest

The authors declare no conflict of interest.

Keywords

biofabrication, cancer models, micro and nanoengineering, microfluidics, tissue engineering, tumor-on-a-chip

Received: January 21, 2023

Revised: April 5, 2023

Published online:

- [1] International Agency for Research on Cancer, "Cancer Tomorrow," <https://gco.iarc.fr/tomorrow/en>, accessed: May, 2022.
- [2] J. E. Visvader, *Nature* **2011**, 469, 314.
- [3] O. Vincze, F. Colchero, J. F. Lemaître, D. A. Conde, S. Pavard, M. Bieuvre, A. O. Urrutia, B. Ujvari, A. M. Boddy, C. C. Maley, F. Thomas, M. Giraudeau, *Nature* **2022**, 601, 263.
- [4] D. Aran, R. Camarda, J. Odegaard, H. Paik, B. Oskotsky, G. Krings, A. Goga, M. Sirota, A. J. Butte, *Nat. Commun.* **2017**, 8, 1077.
- [5] S. Unsal-Beyge, N. Tuncbag, *npj Syst. Biol. Appl.* **2022**, 8, 11.
- [6] A. Clauset, K. Behbakht, B. G. Bitler, *Sci. Adv.* **2021**, 7, eabi5904.
- [7] M. Gerstung, C. Jolly, I. Leshchiner, S. C. Dentro, S. Gonzalez, D. Rosebrock, T. J. Mitchell, Y. Rubanova, P. Anur, K. Yu, M. Tarabichi, A. Deshwar, J. Wintersinger, K. Kleinheinz, I. Vázquez-García, K. Haase, L. Jerman, S. Sengupta, G. Macintyre, S. Malikic, N. Donmez, D. G. Livitz, M. Cmero, J. Demeulemeester, S. Schumacher, Y. Fan, X. Yao, J. Lee, M. Schlesner, P. C. Boutros, et al., *Nature* **2020**, 578, 122.
- [8] B. A. Luca, V. Moulton, C. Ellis, D. R. Edwards, C. Campbell, R. A. Cooper, J. Clark, D. S. Brewer, C. S. Cooper, *Br. J. Cancer* **2020**, 122, 1467.
- [9] J. Fares, M. Y. Fares, H. H. Khachfe, H. A. Salhab, Y. Fares, *Signal Transduction Targeted Ther.* **2020**, 5, 28.
- [10] P. S. Steeg, *Nat. Med.* **2006**, 12, 895.
- [11] H. Dillekås, M. S. Rogers, O. Straume, *Cancer Med.* **2019**, 8, 5574.
- [12] R. Baghban, L. Roshangar, R. Jahanban-Esfahlan, K. Seidi, A. Ebrahimi-Kalan, M. Jaymand, S. Kolahian, T. Javaheri, P. Zare, *Cell Commun. Signaling* **2020**, 18, 59.
- [13] J. Rodrigues, M. A. Heinrich, L. M. Teixeira, J. Prakash, *Trends Cancer* **2021**, 7, 249.
- [14] E. P. Carter, R. Roozitalab, S. V. Gibson, R. P. Grose, *Trends Cancer* **2021**, 7, 1033.
- [15] F. Salaris, A. Rosa, *Brain Res.* **2019**, 1723, 146393.
- [16] D. Rosenblum, N. Joshi, W. Tao, J. M. Karp, D. Peer, *Nat. Commun.* **2018**, 9, 1410.
- [17] S. Nizzero, A. Ziemys, M. Ferrari, *Trends Cancer* **2018**, 4, 277.

- [18] B. Ouyang, W. Poon, Y. N. Zhang, Z. P. Lin, B. R. Kingston, A. J. Tavares, Y. Zhang, J. Chen, M. S. Valic, A. M. Syed, P. MacMillan, J. Couture-Sen  cal, G. Zheng, W. C. W. Chan, *Nat. Mater.* **2020**, *19*, 1362.
- [19] Y. Zhang, J. Yu, H. N. Bomba, Y. Zhu, Z. Gu, *Chem. Rev.* **2016**, *116*, 12536.
- [20] D. C. Hinshaw, L. A. Shevde, *Cancer Res.* **2019**, *79*, 4557.
- [21] S. AlMusawi, M. Ahmed, A. S. Nateri, *Clin. Transl. Med.* **2021**, *11*, e308.
- [22] B. Arneth, *Med* **2020**, *56*, 15.
- [23] M. Z. Jin, W. L. Jin, *Signal Transduction Target Ther.* **2020**, *5*, 67.
- [24] F. R. Balkwill, M. Capasso, T. Hagemann, *J. Cell Sci.* **2012**, *125*, 5591.
- [25] N. M. Anderson, M. C. Simon, *Curr. Biol.* **2020**, *30*, R921.
- [26] R. Burgos-Panadero, F. Lucantoni, E. Gamero-Sandemetrio, L. de la Cruz-Merino, T.   lvoro, R. Noguera, *Cancer Lett.* **2019**, *461*, 112.
- [27] C. Bonnans, J. Chou, Z. Werb, *Nat. Rev. Mol. Cell Biol.* **2014**, *15*, 786.
- [28] R. Zefferino, C. Piccoli, S. Di Gioia, N. Capitanio, M. Conese, *Int. J. Mol. Sci.* **2021**, *22*, 2550.
- [29] B. Emon, J. Bauer, Y. Jain, B. Jung, T. Saif, *Comput. Struct. Biotechnol. J.* **2018**, *16*, 279.
- [30] F. Li, M. C. Simon, *Dev. Cell* **2020**, *54*, 183.
- [31] C. H. Chang, J. Qiu, D. O'Sullivan, M. D. Buck, T. Noguchi, J. D. Curtis, Q. Chen, M. Gindin, M. M. Gubin, G. J. W. Van Der Windt, E. Tonc, R. D. Schreiber, E. J. Pearce, E. L. Pearce, *Cell* **2015**, *162*, 1229.
- [32] Q. Jia, A. Wang, Y. Yuan, B. Zhu, H. Long, *Exp. Hematol. Oncol.* **2022**, *11*, 24.
- [33] L. Guo, D. Kong, J. Liu, L. Zhan, L. Luo, W. Zheng, Q. Zheng, C. Chen, S. Sun, *Exp. Hematol. Oncol.* **2023**, *12*, 3.
- [34] H. Mohammadi, E. Sahai, *Nat. Cell Biol.* **2018**, *20*, 766.
- [35] B. Blanco, H. Gomez, J. Melchor, R. Palma, J. Soler, G. Rus, *Phys. Life Rev.* **2023**, *44*, 279.
- [36] J. M. Northcott, I. S. Dean, J. K. Mouw, V. M. Weaver, *Front. Cell Dev. Biol.* **2018**, *6*, 17.
- [37] R. E. Vickman, D. V. Faget, P. Beachy, D. Beebe, N. A. Bhowmick, E. Cukierman, W.-M. Deng, J. G. Granneman, J. Hildesheim, R. Kalluri, K. S. Lau, E. Lengyel, J. Lundeberg, J. Moscat, P. S. Nelson, K. Pietras, K. Politi, E. Pur  , R. Scherz-Shouval, M. H. Sherman, D. Tuveson, A. T. Weeraratna, R. M. White, M. H. Wong, E. C. Woodhouse, Y. Zheng, S. W. Hayward, S. A. Stewart, *Oncotarget* **2020**, *11*, 3621.
- [38] H. T. Nia, L. L. Munn, R. K. Jain, *Science* **2020**, *370*, 6516.
- [39] X. Liu, J. Fang, S. Huang, X. Wu, X. Xie, J. Wang, F. Liu, M. Zhang, Z. Peng, N. Hu, *Microsystems Nanoeng.* **2021**, *7*, 50.
- [40] C. Jensen, Y. Teng, *Front. Mol. Biosci.* **2020**, *7*, 33.
- [41] S. Melissaridou, E. Wiechec, M. Magan, M. V. Jain, M. K. Chung, L. Farnebo, K. Roberg, *Cancer Cell Int.* **2019**, *19*, 16.
- [42] M. Turetta, F. Del Ben, G. Brisotto, E. Biscontin, M. Bulfoni, D. Ces-selli, A. Colombatti, G. Scoles, G. Gigli, L. L. del Mercato, *Curr. Med. Chem.* **2018**, *25*, 4616.
- [43] S. Gunti, A. T. K. Hoke, K. P. Vu, N. R. London, *Cancers* **2021**, *13*, 874.
- [44] B. L. LeSavage, R. A. Suhar, N. Broguiere, M. P. Lutolf, S. C. Heilshorn, *Nat. Mater.* **2022**, *21*, 143.
- [45] Y. Zhou, W. M. Rideout, T. Zi, A. Bressel, S. Reddypalli, R. Rancourt, J. K. Woo, J. W. Horner, L. Chin, M. I. Chiu, M. Bosenberg, T. Jacks, S. C. Clark, R. A. Depinho, M. O. Robinson, J. Heyer, *Nat. Biotechnol.* **2010**, *28*, 71.
- [46] J. Pape, M. Emberton, U. Cheema, *Front. Bioeng. Biotechnol.* **2021**, *9*, 276.
- [47] W. Sun, Z. Luo, J. Lee, H. J. Kim, K. J. Lee, P. Tebon, Y. Feng, M. R. Dokmeci, S. Sengupta, A. Khademhosseini, *Adv. Healthcare Mater.* **2019**, *8*, 1801363.
- [48] J. C. Fontoura, C. Viezzer, F. G. dos Santos, R. A. Ligabue, R. Weinlich, R. D. Puga, D. Antonow, P. Severino, C. Bonorino, *Mater. Sci. Eng. C* **2020**, *107*, 110264.
- [49] M. A. G. Barbosa, C. P. R. Xavier, R. F. Pereira, V. Petrikait  , M. H. Vasconcelos, *Cancers* **2021**, *14*, 190.
- [50] A. Sontheimer-Phelps, B. A. Hassell, D. E. Ingber, *Nat. Rev. Cancer* **2019**, *19*, 65.
- [51] M. Rahmanian, A. Seyfoori, M. Ghasemi, M. Shamsi, A. R. Kolahchi, H. P. Modarres, A. Sanati-Nezhad, K. Majidzadeh-A, *J. Controlled Release* **2021**, *334*, 164.
- [52] N. Boucherit, L. Gorvel, D. Olive, *Front. Immunol.* **2020**, *11*, 3220.
- [53] M. E. Katt, A. L. Placone, A. D. Wong, Z. S. Xu, P. C. Searson, *Front. Bioeng. Biotechnol.* **2016**, *4*, 12.
- [54] D. V. LaBarbera, B. G. Reid, B. H. Yoo, *Expert Opin. Drug Discovery* **2012**, *7*, 819.
- [55] K. H. Lee, T. H. Kim, *Biosensors* **2021**, *11*, 445.
- [56] S. J. Han, S. Kwon, K. S. Kim, *Cancer Cell Int.* **2021**, *21*, 152.
- [57] T. Bauleth-Ramos, T. Feij  o, A. Gonalves, M. A. Shahbazi, Z. Liu, C. Barrias, M. J. Oliveira, P. Granja, H. A. Santos, B. Sarmento, *J. Controlled Release* **2020**, *323*, 398.
- [58] H. Xu, D. Jiao, A. Liu, K. Wu, *J. Hematol. Oncol.* **2022**, *15*, 104.
- [59] Y. H. Lo, K. Karlsson, C. J. Kuo, *Nat. Cancer* **2020**, *1*, 761.
- [60] M. S. B. Reddy, D. Ponnamma, R. Choudhary, K. K. Sadasivuni, *Polymers* **2021**, *13*, 1105.
- [61] N. A. Pattanashetti, S. Biscaia, C. Moura, G. R. Mitchell, M. Y. Kariduraganavar, *Mater. Today Commun.* **2019**, *21*, 100651.
- [62] J. C. Silva, M. S. Carvalho, R. N. Udangawa, C. S. Moura, J. M. S. Cabral, C. L. da Silva, F. C. Ferreira, D. Vashishth, R. J. Linhardt, *J. Biomed. Mater. Res. – Part B Appl. Biomater.* **2020**, *108*, 2153.
- [63] Y. Lv, H. Wang, G. Li, B. Zhao, *Bioact. Mater.* **2021**, *6*, 2767.
- [64] M. Tamayo-Angorrilla, J. L  pez de Andr  s, G. Jim  nez, J. A. Marchal, *Transl. Res.* **2022**, *247*, 117.
- [65] M. Jung, S. Ghamrawi, E. Y. Du, J. J. Gooding, M. Kavallaris, M. Jung, S. Ghamrawi, M. Kavallaris, E. Y. Du, J. J. Gooding, *Adv. Healthcare Mater.* **2022**, *11*, 2200690.
- [66] P. Datta, M. Dey, Z. Ataie, D. Unutmaz, I. T. Ozbolat, *npj Precis. Oncol* **2020**, *4*, 18.
- [67] G. Trujillo-de Santiago, B. G. Flores-Garza, J. A. Tavares-Negrete, I. M. Lara-Mayorga, I. Gonz  lez-Gamboa, Y. S. Zhang, A. Rojas-Martinez, R. Ortiz-L  pez, M. M.   lvarez, *Materials* **2019**, *12*, 2945.
- [68] L. K. Chim, A. G. Mikos, *Curr. Opin. Biomed. Eng.* **2018**, *6*, 42.
- [69] P. K. Chaudhuri, B. C. Low, C. T. Lim, *Chem. Rev.* **2018**, *118*, 6499.
- [70] R. C. Oliveira, A. M. Abrantes, J. G. Tralh  o, M. F. Botelho, *Anim. Models Exp. Med.* **2020**, *3*, 1.
- [71] D. Eastwood, L. Findlay, S. Poole, C. Bird, M. Wadhwa, M. Moore, C. Burns, R. Thorpe, R. Stebbings, *Br. J. Pharmacol.* **2010**, *161*, 512.
- [72] S. K. Sarvestani, R. K. DeHaan, P. G. Miller, S. Bose, X. Shen, M. L. Shuler, E. H. Huang, *iScience* **2020**, *23*, 101719.
- [73] M. A. Heinrich, A. M. R. H. Mostafa, J. P. Morton, L. J. A. C. Hawinkels, J. Prakash, *Adv. Drug Delivery Rev.* **2021**, *174*, 265.
- [74] X. Sol  -Mart  , A. Espona-Noguera, M. P. Ginebra, C. Canal, *Cancers* **2021**, *13*, 452.
- [75] T. Murayama, N. Gotoh, *Cells* **2019**, *8*, 621.
- [76] J. Hoarau-V  chet, A. Rafii, C. Touboul, J. Pasquier, *Int. J. Mol. Sci.* **2018**, *19*, 181.
- [77] F. Fontana, P. Figueiredo, J. P. Martins, H. A. Santos, *Small* **2021**, *17*, 2004182.
- [78] K. D'Costa, M. Kopic, A. Lam, A. Moradipour, Y. Zhao, M. Radisic, *Ann. Biomed. Eng.* **2020**, *48*, 2002.
- [79] N. Moghimi, S. A. Hosseini, M. Poudineh, M. Kohandel, *Int. J. Bio-print.* **2022**, *28*, e00238.
- [80] D. Hanahan, R. A. Weinberg, *Cell* **2000**, *100*, 57.
- [81] S. A. Aaronson, *Science* **1991**, *254*, 1146.
- [82] J. Komen, S. M. van Neerven, A. van den Berg, L. Vermeulen, A. D. van der Meer, *EBioMedicine* **2021**, *66*, 103303.
- [83] S. Parlato, G. Grisanti, G. Sinibaldi, G. Peruzzi, C. M. Casciola, L. Gabriele, *Lab Chip* **2021**, *21*, 234.
- [84] Z. Ao, H. Cai, Z. Wu, L. Hu, X. Li, C. Kaurich, M. Gu, L. Cheng, X. Lu, F. Guo, *Theranostics* **2022**, *12*, 3628.

- [85] S. Bërziqja, A. Harrison, V. Taly, W. Xiao, *Cancers* **2021**, *13*, 4192.
- [86] M. Bavoux, Y. Kamio, E. Vigneux-Foley, J. Lafontaine, O. Najyb, E. Refet-Mollof, J. F. Carrier, T. Gervais, P. Wong, *Radiother. Oncol.* **2021**, *157*, 175.
- [87] S. Mao, Y. Pang, T. Liu, Y. Shao, J. He, H. Yang, Y. Mao, W. Sun, *Biofabrication* **2020**, *12*, 042001.
- [88] A. E. Danku, E. H. Dulf, C. Braicu, A. Jurj, I. Berindan-Neagoe, *Front. Bioeng. Biotechnol.* **2022**, *10*, 94.
- [89] S. Ahmed, V. M. Chauhan, A. M. Ghaemmaghami, J. W. Aylott, *Biotechnol. Lett.* **2019**, *41*, 1.
- [90] S. Ullah, X. Chen, *Appl. Mater. Today* **2020**, *20*, 100656.
- [91] M. Abbasian, B. Massoumi, R. Mohammad-Rezaei, H. Samadian, M. Jaymand, *Int. J. Biol. Macromol.* **2019**, *134*, 673.
- [92] B. Saha, T. Mathur, J. J. Tronolone, M. Chokshi, G. K. Lokhande, A. Selahi, A. K. Gaharwar, V. Afshar-Kharghan, A. K. Sood, G. Bao, A. Jain, *Sci. Adv.* **2021**, *7*, 5283.
- [93] Z. Li, D. Li, Y. Guo, Y. Wang, W. Su, *Biotechnol. Lett.* **2021**, *43*, 383.
- [94] J. Lee, S. E. Kim, D. Moon, J. Doh, *Lab Chip* **2021**, *21*, 2142.
- [95] X. Cao, R. Ashfaq, F. Cheng, S. Maharjan, J. Li, G. Ying, S. Hassan, H. Xiao, K. Yue, Y. S. Zhang, *Adv. Funct. Mater.* **2019**, *29*, 1807173.
- [96] G. Miserocchi, L. Mercatali, C. Liverani, A. De Vita, C. Spadazzi, F. Pieri, A. Bongiovanni, F. Recine, D. Amadori, T. Ibrahim, *J. Transl. Med.* **2017**, *15*, 229.
- [97] V. Foglizzo, E. Cocco, S. Marchiò, *Cancers* **2022**, *14*, 3692.
- [98] F. Janku, *Ther. Adv. Med. Oncol.* **2014**, *6*, 43.
- [99] A. Wnorowski, H. Yang, J. C. Wu, *Adv. Drug Delivery Rev.* **2019**, *140*, 3.
- [100] A. Johnson, S. Reimer, R. Childres, G. Cupp, T. C. L. Kohs, O. J. T. McCarty, Y. (A.) Kang, *Cell. Mol. Bioeng.* **2022**, *1*.
- [101] J. A. De Lora, J. L. Velasquez, N. J. Carroll, J. P. Freyer, A. P. Shreve, *SLAS Technol* **2020**, *25*, 436.
- [102] V. Velasco, S. A. Shariati, R. Esfandyarpour, *Microsyst. Nanoeng.* **2020**, *6*, 76.
- [103] N. E. Timmins, L. K. Nielsen, *Methods Mol. Med.* **2007**, *140*, 141.
- [104] E. C. Costa, D. de Melo-Diogo, A. F. Moreira, M. P. Carvalho, I. J. Correia, *Biotechnol. J.* **2018**, *13*, 1700417.
- [105] D. Tuveson, H. Clevers, *Science* **2019**, *364*, 952.
- [106] T. Xia, W. L. Du, X. Y. Chen, Y. N. Zhang, *J. Cell. Mol. Med.* **2021**, *25*, 5829.
- [107] V. Carvalho, M. Bañobre-López, G. Minas, S. F. C. F. Teixeira, R. Lima, R. O. Rodrigues, *Int. J. Bioprint.* **2022**, *27*, e00224.
- [108] S. Santoni, S. G. Gugliandolo, M. Sponchioni, D. Moscatelli, B. M. Colosimo, *Bio-Design Manuf.* **2022**, *5*, 14.
- [109] D. V. Leonov, Y. A. Spirina, A. A. Yatsenko, V. A. Kushnarev, E. M. Ustinov, S. V. Barannikov, *Cell Tissue Biol.* **2021**, *15*, 616.
- [110] S. G. Anthon, K. P. Valente, *Int. J. Mol. Sci.* **2022**, *23*, 14582.
- [111] H. G. Yi, Y. H. Jeong, Y. Kim, Y. J. Choi, H. E. Moon, S. H. Park, K. S. Kang, M. Bae, J. Jang, H. Youn, S. H. Paek, D. W. Cho, *Nat. Biomed. Eng.* **2019**, *3*, 509.
- [112] C. Mazzaglia, Y. Sheng, L. N. Rodrigues, I. M. Lei, J. D. Shields, Y. Y. S. Huang, *bioRxiv* **2022**, <https://doi.org/10.1101/2022.04.08.487692>.
- [113] N. Dhirman, N. Shagaghi, M. Bhavne, H. Sumer, P. Kingshott, S. N. Rath, *Cytotherapy* **2021**, *23*, 25.
- [114] S. S. Kumar, presented at *Int. Young Res. Conf., Vir*, Virtual, June **2021**.
- [115] A. D. Rodriguez, L. F. Horowitz, K. Castro, H. Kenerson, N. Bhat-tarjee, G. Gandhe, A. Raman, R. J. Monnat, R. Yeung, R. C. Ros-tomily, A. Folch, *Lab Chip* **2020**, *20*, 1658.
- [116] F. Olubajo, S. Achawal, J. Greenman, *Transl. Oncol.* **2020**, *13*, 1.
- [117] J. Ko, J. Ahn, S. Kim, Y. Lee, J. Lee, D. Park, N. L. Jeon, *Lab Chip* **2019**, *19*, 2822.
- [118] Y. Xiao, D. Kim, B. Dura, K. Zhang, R. Yan, H. Li, E. Han, J. Ip, P. Zou, J. Liu, A. T. Chen, A. O. Vortmeyer, J. Zhou, R. Fan, *Adv. Sci.* **2019**, *6*, 1801531.
- [119] Y. Bi, V. S. Shirure, R. Liu, C. Cunningham, L. Ding, J. M. Meacham, S. P. Goedegebuure, S. C. George, R. C. Fields, *Integr. Biol.* **2020**, *12*, 221.
- [120] M. R. Carvalho, D. Barata, L. M. Teixeira, S. Giselbrecht, R. L. Reis, J. M. Oliveira, R. Truckenmüller, P. Habibovic, *Sci. Adv.* **2019**, *5*, eaaw1317.
- [121] Y. Asaumi, N. Sasaki, *Sensors Mater.* **2021**, *33*, 241.
- [122] L. Wan, J. Yin, J. Skoko, R. Schwartz, M. Zhang, P. R. LeDuc, C. A. Neumann, *Mol. Cancer Ther.* **2021**, *20*, 1210.
- [123] V. Palacio-castañeda, S. Dumas, P. Albrecht, T. J. Wijgers, S. Des-croix, W. P. R. Verdurmen, *Cancers* **2021**, *13*, 2461.
- [124] J. M. Ayuso, S. Rehman, M. Virumbrales-Munoz, P. H. McMinn, P. Geiger, C. Fitzgerald, T. Heaster, M. C. Skala, D. J. Beebe, *Sci. Adv.* **2021**, *7*, eabc2331.
- [125] S. Mi, Z. Liu, Z. Du, X. Yi, W. Sun, *Biotechnol. Bioeng.* **2019**, *116*, 1731.
- [126] M. Nguyen, A. De Ninno, A. Mencattini, F. Mermet-Meillon, G. Forn-abaio, S. S. Evans, M. Cossutta, Y. Khira, W. Han, P. Sirven, F. Pelon, D. Di Giuseppe, F. R. Bertani, A. Gerardino, A. Yamada, S. Descroix, V. Soumelis, F. Mechta-Grigoriou, G. Zalcmán, J. Camonis, E. Mar-tinelli, L. Businaro, M. C. Parrini, *Cell Rep.* **2018**, *25*, 3884.
- [127] J. Song, A. Miermont, C. T. Lim, R. D. Kamm, *Sci. Rep.* **2018**, *8*, 17949.
- [128] Y. C. Toh, A. Raja, H. Yu, D. Van Noort, *Bioengineering* **2018**, *5*, 29.
- [129] C. P. Miller, C. Tsuchida, Y. Zheng, J. Himmelfarb, S. Akilesh, *Neoplasia* **2018**, *20*, 610.
- [130] J. H. Lee, S. K. Kim, I. A. Khawar, S. Y. Jeong, S. Chung, H. J. Kuh, *J. Exp. Clin. Cancer Res.* **2018**, *37*, 4.
- [131] C. Li, S. Li, K. Du, P. Li, B. Qiu, W. Ding, *ACS Appl. Mater. Interfaces* **2021**, *13*, 19768.
- [132] J. D. Lang, S. M. Berry, G. L. Powers, D. J. Beebe, E. T. Alarid, *Integr. Biol.* **2013**, *5*, 807.
- [133] S. Kim, H. Lee, M. Chung, N. L. Jeon, *Lab Chip* **2013**, *13*, 1489.
- [134] K. E. Sung, N. Yang, C. Pehlke, P. J. Keely, K. W. Eliceiri, A. Friedl, D. J. Beebe, *Integr. Biol.* **2011**, *3*, 439.
- [135] S. I. Montanez-Sauri, K. E. Sung, E. Berthier, D. J. Beebe, *Integr. Biol.* **2013**, *5*, 631.
- [136] Y. Xia, G. M. Whitesides, *Annu. Rev. Mater. Sci.* **1998**, *28*, 153.
- [137] V. Silverio, S. C. de Freitas, in *Complex Fluid-Flows Microfluid*, Springer International Publishing, New York, USA **2017**, pp. 25–51.
- [138] B. Erdogan, M. Ao, L. M. White, A. L. Means, B. M. Brewer, L. Yang, M. K. Washington, C. Shi, O. E. Franco, A. M. Weaver, S. W. Hayward, D. Li, D. J. Webb, *J. Cell Biol.* **2017**, *216*, 3799.
- [139] M. B. Chen, J. A. Whisler, J. S. Jeon, R. D. Kamm, *Integr. Biol.* **2013**, *5*, 1262.
- [140] P. Koltay, J. Ducreé, R. D. Zengerle, in *BioMEMS*, Springer, New York, USA **2006**, pp. 139–165.
- [141] V. Silverio, P. A. G. Canane, S. Cardoso, *Colloids Surf., A* **2019**, *570*, 210.
- [142] J. W. Song, S. P. Cavnar, A. C. Walker, K. E. Luker, M. Gupta, Y.-C. Tung, G. D. Luker, S. Takayama, *PLoS One* **2009**, *4*, e5756.
- [143] E. Berthier, D. J. Beebe, *Lab Chip* **2007**, *7*, 1475.
- [144] S. Wang, E. Li, Y. Gao, Y. Wang, Z. Guo, J. He, J. Zhang, Z. Gao, Q. Wang, *PLoS One* **2013**, *8*, e56448.
- [145] M. Ao, B. M. Brewer, L. Yang, O. E. Franco Coronel, S. W. Hayward, D. J. Webb, D. Li, *Sci. Rep.* **2015**, *5*, 8334.
- [146] X. Wang, D. T. T. Phan, A. Sobrino, S. C. George, C. C. W. Hughes, A. P. Lee, *Lab Chip* **2016**, *16*, 282.
- [147] M. Radisic, P. Loskill, *ACS Biomater. Sci. Eng.* **2021**, *7*, 2861.
- [148] I. Rizvi, U. A. Gurkan, S. Tasoglu, N. Alagic, J. P. Celli, L. B. Mensah, Z. Mai, U. Demirci, T. Hasan, *Proc. Natl. Acad. Sci. USA* **2013**, *110*, E1974.
- [149] W. Asghar, M. Yuksekkaya, H. Shafiee, M. Zhang, M. O. Ozen, F. Inci, M. Kocakulak, U. Demirci, *Sci. Rep.* **2016**, *6*, 21163.

- [150] M. Kim, Y. Alapan, A. Adhikari, J. A. Little, U. A. Gurkan, *Microcirculation* **2017**, *24*, e12374.
- [151] M. Sher, B. Coleman, M. Caputi, W. Asghar, *Sensors* **2021**, *21*, 1819.
- [152] L. Wan, J. Skoko, J. Yu, P. R. Leduc, C. A. Neumann, *Sci. Rep.* **2017**, *7*, 16724.
- [153] M. Wang, X. Yang, L. Liang, *J. Chem.* **2020**, *2020*, 3148652.
- [154] K. ichiro Kamei, Y. Mashimo, Y. Koyama, C. Fockenber, M. Nakashima, M. Nakajima, J. Li, Y. Chen, *Biomed. Microdevices* **2015**, *17*, 1.
- [155] A. Chiadò, G. Palmara, A. Chiappone, C. Tanzanu, C. F. Pirri, I. Ropolo, F. Frascella, *Lab Chip* **2020**, *20*, 665.
- [156] T. H. Hsu, J. L. Xiao, Y. W. Tsao, Y. L. Kao, S. H. Huang, W. Y. Liao, C. H. Lee, *Lab Chip* **2011**, *11*, 1808.
- [157] B. A. Hassell, G. Goyal, E. Lee, A. Sontheimer-Phelps, O. Levy, C. S. Chen, D. E. Ingber, *Cell Rep.* **2017**, *21*, 508.
- [158] M. Jang, P. Neuzil, T. Volk, A. Manz, A. Kleber, *Biomicrofluidics* **2015**, *9*, 034113.
- [159] S. J. Trietsch, G. D. Israëls, J. Joore, T. Hankemeier, P. Vulto, *Lab Chip* **2013**, *13*, 3548.
- [160] L. L. Bischel, D. J. Beebe, K. E. Sung, *BMC Cancer* **2015**, *15*, 12.
- [161] D. H. T. Nguyen, S. C. Stapleton, M. T. Yang, S. S. Cha, C. K. Choi, P. A. Galie, C. S. Chen, *Proc. Natl. Acad. Sci. USA* **2013**, *110*, 6712.
- [162] J. M. Ayuso, R. Truttschel, M. M. Gong, M. Humayun, M. Virumbrales-Munoz, R. Vitek, M. Felder, S. D. Gillies, P. Sondel, K. B. Wisinski, M. Patankar, D. J. Beebe, M. C. Skala, *Oncotimmunology* **2019**, *8*, 1553477.
- [163] J. Yeste, X. Illa, M. Alvarez, R. Villa, *J. Biol. Eng.* **2018**, *12*, 18.
- [164] D. Huh, B. D. Matthews, A. Mammoto, M. Montoya-Zavala, H. Y. Hsin, D. E. Ingber, *Science* **2010**, *328*, 1662.
- [165] W. Shin, C. D. Hinojosa, D. E. Ingber, H. J. Kim, *iScience* **2019**, *15*, 391.
- [166] T. H. Hsu, Y. L. Kao, W. L. Lin, J. L. Xiao, P. L. Kuo, C. W. Wu, W. Y. Liao, C. H. Lee, *Integr. Biol.* **2012**, *4*, 177.
- [167] Y. Feng, B. Wang, Y. Tian, H. Chen, Y. Liu, H. Fan, K. Wang, C. Zhang, *Biosens. Bioelectron.* **2020**, *151*, 111966.
- [168] K. L. Fetah, B. J. DiPardo, E. M. Kongadzem, J. S. Tomlinson, A. Elzagheid, M. Elmusrati, A. Khademhosseini, N. Ashammakhi, *Small* **2019**, *15*, 1901985.
- [169] F. Alexander, S. Eggert, J. Wiest, *Cytotechnology* **2018**, *70*, 375.
- [170] F. Liebisch, A. Weltin, J. Marzioch, G. A. Urban, J. Kieninger, *Sens. Actuators, B* **2020**, *322*, 128652.
- [171] C. Fang, F. Ji, Z. Shu, D. Gao, *Lab Chip* **2017**, *17*, 951.
- [172] Q. Wu, X. Wei, Y. Pan, Y. Zou, N. Hu, P. Wang, *Biomed. Microdevices* **2018**, *20*, 33.
- [173] Y. R. F. Schmid, S. C. Bürgel, P. M. Misun, A. Hierlemann, O. Frey, *ACS Sens.* **2016**, *1*, 1028.
- [174] P. M. Misun, J. Rothe, Y. R. F. Schmid, A. Hierlemann, O. Frey, *Microsyst. Nanoeng.* **2016**, *2*, 16022.
- [175] S. Mi, J. Xia, Y. Xu, Z. Du, W. Sun, *RSC Adv.* **2019**, *9*, 9006.
- [176] A. Weltin, S. Hammer, F. Noor, Y. Kaminski, J. Kieninger, G. A. Urban, *Biosens. Bioelectron.* **2017**, *87*, 941.
- [177] Y. S. Zhang, J. Aleman, S. R. Shin, T. Kilic, D. Kim, S. A. M. Shaegh, S. Massa, R. Riahi, S. Chae, N. Hu, H. Avci, W. Zhang, A. Silvestri, A. S. Nezhad, A. Manbohi, F. De Ferrari, A. Polini, G. Calzone, N. Shaikh, P. Alerasool, E. Budina, J. Kang, N. Bhise, J. Ribas, A. Pourmand, A. Skardal, T. Shupe, C. E. Bishop, M. R. Dokmeci, A. Atala, et al., *Proc. Natl. Acad. Sci. USA* **2017**, *114*, E2293.
- [178] S. Cruz, A. Girão, G. Gonçalves, P. Marques, *Sensors* **2016**, *16*, 137.
- [179] A. Rodríguez-Pena, J. Uranga-Solchaga, C. Ortiz-de-Solórzano, I. Cortés-Domínguez, *Sci. Rep.* **2020**, *10*, 2779.
- [180] P. Paiè, R. Martínez Vázquez, R. Osellame, F. Bragheri, A. Bassi, *Cytometry, Part A* **2018**, *93*, 987.
- [181] Z. Zhang, L. Chen, Y. Wang, T. Zhang, Y. C. Chen, E. Yoon, *Anal. Chem.* **2019**, *91*, 14093.
- [182] M. S. Jeon, Y. Y. Choi, S. J. Mo, J. H. Ha, Y. S. Lee, H. U. Lee, S. D. Park, J.-J. Shim, J.-L. Lee, B. G. Chung, *Nano Converg.* **2022**, *9*, 8.
- [183] K. C. Chaw, M. Manimaran, E. H. Tay, S. Swaminathan, *Lab Chip* **2007**, *7*, 1041.
- [184] C. Strelez, S. Chilakala, K. Ghaffarian, R. Lau, E. Spiller, N. Ung, D. Hixon, A. Y. Yoon, R. X. Sun, H. J. Lenz, J. E. Katz, S. M. Mumenthaler, *iScience* **2021**, *24*, 5.
- [185] M. Marzagalli, G. Pelizzoni, A. Fedi, C. Vitale, F. Fontana, S. Bruno, A. Poggi, A. Dondero, M. Aiello, R. Castriconi, C. Bottino, S. Scaglione, *Front. Bioeng. Biotechnol.* **2022**, *10*, 1283.
- [186] C. W. Chi, Y. H. Lao, A. H. R. Ahmed, E. C. Benoy, C. Li, Z. Dereli-Korkut, B. M. Fu, K. W. Leong, S. Wang, *Adv. Healthcare Mater.* **2020**, *9*, 2000880.
- [187] H. F. Wang, R. Ran, Y. Liu, Y. Hui, B. Zeng, D. Chen, D. A. Weitz, C. X. Zhao, *ACS Nano* **2018**, *12*, 11600.
- [188] V. Surendran, D. Rutledge, R. Colmon, A. Chandrasekaran, *Biofabrication* **2021**, *13*, 035029.
- [189] Z. Xu, E. Li, Z. Guo, R. Yu, H. Hao, Y. Xu, Z. Sun, X. Li, J. Lyu, Q. Wang, *ACS Appl. Mater. Interfaces* **2016**, *8*, 25840.
- [190] J. H. Sung, C. Kam, M. L. Shuler, *Lab Chip* **2010**, *10*, 446.
- [191] X. Jiang, L. Ren, P. Tebon, C. Wang, X. Zhou, M. Qu, J. Zhu, H. Ling, S. Zhang, Y. Xue, Q. Wu, P. Bandaru, J. Lee, H. J. Kim, S. Ahadian, N. Ashammakhi, M. R. Dokmeci, J. Wu, Z. Gu, W. Sun, A. Khademhosseini, *Small* **2021**, *17*, 2004282.
- [192] Y. Hou, X. Ai, L. Zhao, Z. Gao, Y. Wang, Y. Lu, P. Tu, Y. Jiang, *Lab Chip* **2020**, *20*, 2482.
- [193] Z. Lin, G. Luo, W. Du, T. Kong, C. Liu, Z. Liu, *Small* **2020**, *16*, 1903899.
- [194] H. Y. Cho, J. H. Choi, J. Lim, S. N. Lee, J. W. Choi, *Cancers* **2021**, *13*, 1385.



Vania Silverio is Senior Researcher at INESC Microsistemas e Nanotecnologias, where she leads the Microfluidics Group focusing on strategies to better understand and/or provide microfluidic flow. She is an Invited Assistant Professor in the Department of Physics of Instituto Superior Técnico, ULisboa. She is currently involved in scientifically innovative and challenging projects combining nanotechnology with simulation tools for designing, micro/nanofabricating, integrating, and testing microfluidic platforms, lab-on-chip, and organ-on-chip. She is an expert in the definition of standards and processes for microfluidics (ISO/TC 48/WG 3 – Microfluidic Devices) and is a member of The Microfluidic Association, EUROoCS, IEEE Society USA, EPS, SPF, and IOP. She holds a Ph.D. in mechanical engineering (Tecnico, ULisboa) and a Licenciatura in Technological Chemistry (5 years, FCUL, ULisboa).



Gil Gonçalves graduated in chemistry and received his Ph.D. in mechanical engineering at the University of Aveiro. In 2016, he started working at the Institute of Material Science of Barcelona (ICMAB-CSIC) on neutron capture therapy. He was a short-term visitor at the Laboratory of Applied Nuclear Energy–University of Pavia and at the Department of Chemical and Pharmaceutical Sciences, University of Trieste. He is currently leading a research group at the Center for Mechanical Technology and Automation (TEMA-UA) that is working on innovative nanocomposite materials for cancer therapy and bioimaging, as well as the micro–nanofabrication of tumors on-chip.



Hélder A. Santos (D.Sc. Tech., Chem. Eng.) is a Full Professor at the Department of Biomedical Engineering and Head of the Department of Biomedical Engineering both at the University Medical Center Groningen, University of Groningen. He is also the Chairman and co-founder of Capsamedix Oy, and Coordinator of the H2020 EU MSCA-ITN P4 FIT network. His research interests include the development of nanoparticles/nanomedicines and biomaterials for biomedical applications, particularly cancer and heart diseases. His lab makes the unique bridge between medical engineering and tissue engineering by combining unique techniques to develop novel therapeutic formulations for translation into the clinic.